Industrial Air Toxicant Exposure and Individual Mortality: Evidence from the Americans' Changing Lives Cohort, 1986–2019

Reed T. DeAngelis, PhD [1, *]

Lindsey Burnside, PhD [1]

David Rigby, PhD [1]

Paul Mohai, PhD [1, 2]

Devon Payne-Sturges, MPH, PhD [3]

Margaret T. Hicken, PhD [1]

[1] Institute for Social Research, University of Michigan, Ann Arbor, MI
[2] School for Environment and Sustainability, University of Michigan, Ann Arbor, MI
[3] Department of Environmental Health Sciences, University of Michigan, Ann Arbor, MI

*Corresponding Author: Reed T. DeAngelis, PhD, Institute for Social Research, University of Michigan, 426 Thompson St., Ann Arbor, MI 48104 (rdeangel@umich.edu)

Words: 4,322
References: 63
Tables: 3 main; 8 supplementary
Figures: 3 main; 4 supplementary

Conflicts of Interest
None declared.

Source of Funding
Reed DeAngelis, Lindsey Burnside, David Rigby, Paul Mohai, and Margaret Hicken acknowledge the following funding source: National Institute on Minority Health and Health Disparities (5R01MD016244; PI Hicken).

Data Availability Statement
Deidentified survey data from the Americans' Changing Lives (ACL) study are publicly accessible via the Inter-university Consortium for Political and Social Research (ICPSR; https://www.icpsr.umich.edu, accessed on 28 July 2025). Deidentified geospatial data from the ACL study are publicly accessible via the virtual data enclave of the ICPSR (https://www.icpsr.umich.edu/web/pages/ICPSR/access/restricted/enclave.html, accessed on 28 July 2025).

ABSTRACT

Exposure to industrial air toxicants remains a leading environmental health risk in the United States (US). Our prospective cohort study examines the extent to which industrial air toxicant exposure accounts for individual mortality risk throughout the adult life course. Individual data come from Americans' Changing Lives, a nationally representative US cohort who were followed for six waves between 1986 and 2019 (N = 3,329). Industrial air toxicant data come from the Environmental Protection Agency's Risk-Screening Environmental Indicators Geographic Microdata; toxicants are recorded at each wave within five circular buffers surrounding respondents' homes at increasing radiuses (1-km to 25-km). We employ accelerated failure time-shared frailty survival models that account for unmeasured between-person differences in mortality risk, and other individual- and area-level characteristics measured over time. We report three key findings. First, associations between air toxicants and mortality are non-linear, such that respondents who reside in areas with relatively low toxicant levels still live for ~1-2 fewer years, on average, compared to peers residing in the least polluted areas. Second, toxicants recorded within larger areas approximating the size of cities account for the widest mortality gaps. For example, respondents who reside within the most polluted 25-km buffers during the study period live for ~4 fewer years, on average, compared to their peers in the least polluted areas. Third, several of these associations are amplified for respondents who identify as non-Hispanic Black (vs. White), report lower incomes, or reside in high-poverty census tracts. Our study corroborates that industrial air toxicants remain significant environmental health risks in the US, especially for socioeconomically disadvantaged populations.

KEYWORDS

air toxicants; Americans' Changing Lives; differential vulnerability; industrial pollution; mortality; Risk Screening Environmental Indicators Geographic Microdata (RSEI-GM)

INTRODUCTION

Despite decades of successful environmental regulations and air quality improvements in the United States (US), exposure to industrial air pollution remains a leading environmental health risk.[1,2] By recent estimates, 100,000 annual US deaths are attributable to anthropogenic emissions, broadly, with one-third linked specifically to industrial emissions.[1] Dozens of epidemiological cohort studies conducted over the past thirty years have also uncovered robust links between air pollution exposure and all-cause, cardiopulmonary, and lung cancer mortality.[3] Moreover, studies have revealed elevated mortality risks even among populations exposed to relatively low pollution levels, suggesting there may be no safe exposure threshold.[4,5]

Our study offers several novel contributions to this literature. First, we assess links between industrial air toxicants and mortality risk among over 3,000 participants in the Americans' Changing Lives (ACL) study, a diverse and national longitudinal cohort that has been followed for six waves from 1986 to 2019.[6,7] The ACL study offers a unique opportunity to incorporate into our mortality estimates historically high industrial toxicant levels that predate critical environmental regulations of the 1990s.[8,9] Exploiting the multilevel and longitudinal structure of the ACL data, we can also account for unmeasured between-person differences in mortality risk, and a battery of individual- and area-level characteristics measured over time.

Second, studies typically employ area-level proxies of pollution exposure that do not account for multiple spatial scales or pollutant toxicity levels.[2] We address these limitations by modeling repeat toxicant concentrations at five spatial scales using the Environmental Protection Agency's (EPA) Risk-Screening Environmental Indicators Geographic Microdata (RSEI-GM).[10–12] The RSEI-GM database includes granular air toxicant measures that quantify the differential toxicity of industrial pollutants based on their known capacity to cause chronic health conditions like cancer.[10] While several studies have linked RSEI-GM indicators to individual-level health outcomes,[13–15] no study we know of has examined links with individual mortality among a diverse national cohort.

Third, owing to the diversity of the ACL cohort, our study is also uniquely situated for testing the *differential vulnerability hypothesis*. Broadly, this hypothesis predicts that the adverse health effects of industrial

toxicant exposure will be amplified for otherwise vulnerable or distressed populations.[16–18] For example, people with lower incomes are vulnerable to chronic financial stress,[19] and often lack access to healthful resources like high-quality nutrition, healthcare, and exercise facilities.[20] Relative to their White peers, Black and Hispanic Americans also tend to report more health complications from psychosocial stressors, including financial strain, traumatic life events, and unfair treatment.[21–25] Moreover, racialized health disparities often persist even when Black and Hispanic Americans achieve higher socioeconomic status (SES).[26–30] Together, these findings suggest that chronic socioeconomic deprivation and stress could exacerbate the adverse health effects of air toxicant exposure for disadvantaged socioeconomic and racial-ethnic groups.

Due to generations of institutionalized segregation (e.g., redlining), residential areas across the United States also remain starkly segregated by race-ethnicity and SES. [31,32] Residential areas characterized by concentrated disadvantage, including disproportionate shares of residents in poverty or from minoritized racial-ethnic backgrounds, often contain other hazards aside from air pollution, such as social disorder;[33,34] police brutality;[35] water and soil pollution; [36,37] and lack of food retailers, greenspace, and other infrastructure conducive to resident health.[38–40] In turn, prolonged exposure to neighborhood contexts like these could generate chronic proinflammatory stress responses and cardiometabolic dysregulation,[41–43] ultimately interacting with and compounding the adverse health effects of air toxicant exposure.

Despite mixed results,[44,45] studies have found that the associations between pollution exposure and morbidity or mortality are larger for Black (vs. White) Americans,[16,46] lower-income groups,[46] and groups exposed to more stressors.[18] Studies have also found that states with more income inequality and/or Black residents exhibit stronger associations between state-level particulate matter and diminished resident life expectancy, relative to peer states with lower income inequality and/or smaller Black populations.[47,48]

The differential vulnerability hypothesis ultimately reflects a stress-moderating process.[19] To test this hypothesis, we examine whether associations between RSEI-GM air toxicant indicators and mortality are amplified for respondents who identify as Black or Hispanic (vs. White), report lower incomes, or reside in

racially segregated or high-poverty areas. These additional characteristics of respondents and their residential contexts are meant to proxy other latent environmental conditions we cannot measure directly.

METHODS

Americans' Changing Lives (ACL) Study

Individual data include Waves 1 through 6 of the ACL study, a closed longitudinal cohort study following a national sample of 3,618 adults in the contiguous US. ACL was approved by the University of Michigan's Institutional Review Board (#HUM00153243). All respondents provided written informed consent before participating in any wave. ACL recruited respondents from a multistage stratified area probability sample, including oversamples of Black and older-age adults, resulting in a baseline sample of adults ages 25 to 96 with a mean age of 54 in 1986.[6] ACL reinterviewed respondents in 1989, 1994, 2001-2002, 2011, and 2019. Relevant to our study, geocoordinates of respondents' residential locations are recorded at each wave. ACL also conducts regular mortality tracking between waves using the National Death Index (NDI).[50] Our analytic sample includes respondents with no missing observations at Wave 1 (N = 3,329).

Risk-Screening Environmental Indicators Geographic Microdata (RSEI-GM)

Industrial air toxicant data come from RSEI-GM.[10–12] RSEI-GM is modeled from data on air releases and transfers reported by every facility in the EPA's Toxics Release Inventory (TRI). RSEI-GM models account for the fate of pollutants based on inputs like the total amounts of emitted pollutants, their sources of release (e.g., smokestack), molecular weights and decay rates, and local weather and topography. Our measures also incorporate toxicity weights applied to each pollutant, a.k.a., "toxicity-weighted concentrations." Toxicity weights are relative numerical ranks based on the known potential for different pollutants to cause chronic health conditions from long-term exposure (e.g., cancer). Thus, toxicity-weighted concentrations are designed to gauge chronic human toxicity associated with long-term exposure to industrial air toxicants.[51]

The EPA has released RSEI-GM data annually since 1988. In our study, respondents' residential locations are linked to toxicants recorded one year before their interviews. For instance, because Wave 2

occurred throughout the year 1989, respondent locations are linked with the first RSEI-GM dataset released in 1988. Starting in 1995, the EPA also began making major updates to the TRI list to include additional chemicals and industrial facilities, while maintaining a list of ~300 core chemicals from 1988. Our measures reflect toxicity-weighted concentrations of chemicals included in the original 1988 core chemical list.

Because ACL started in 1986, respondents at Wave 1 are also linked to the earliest RSEI-GM database in 1988. According to historical EPA data, national averages of industrial air emissions were relatively stable between Waves 1 and 2 of ACL. For example, estimates of total suspended particulate from industrial processes were 2.5 and 2.7 million metric tons in 1986 and 1989, respectively.[52] As other scholars have already documented, levels of industrial air pollution did not begin to drastically change until after the passing of new EPA regulations in 1990.[8,9] Thus, we assume that levels of industrial air toxicants in 1986 were comparable to those first documented in 1988. Still, we acknowledge this as a data limitation, and address it by controlling for respondents' patterns of residential mobility across waves (see below).

Using geospatial packages in *R* and *PySpark*, we merged RSEI-GM toxicity-weighted concentrations into all waves of ACL through a multistep process. First, we created five circular buffers around respondents' residences at radiuses of 1-km, 2-km, 5-km, 10-km, and 25-km. Second, we created a new database containing the geometric intersections of the five circular buffers with the RSEI-GM grid system, which is composed of 810 meters by 810 meters square grid cells. In this merged database, we then calculated the land area proportions of RSEI-GM square grid cells that overlapped with the five circular buffers. Next, we spatially weighted the toxicity-weighted concentrations recorded in RSEI-GM square grid cells, multiplying grid concentrations by their respective proportions of land area contained within each of the five circular buffers. Finally, we aggregated toxicity-weighted concentrations to the circular buffer level by averaging all spatially weighted RSEI-GM square grid concentrations contained within each circular buffer. The result is a set of toxicity-weighted concentrations within five circular buffers surrounding respondents' residential addresses at increasing radiuses (1-km to 25-km). The five buffers are meant to gauge air toxicant exposures within residential contexts and broader activity spaces (e.g., daily commutes, leisure sites, etc.).

Measurement

Mortality. Mortality data originate from causes of death reported on participants' death certificates. Causes of death are categorized according to ICD-9 and ICD-10 codes (International Classification of Diseases, 9th and 10th revisions, respectively). Mortality data are summarized in Table 1 and Figure S1 (online supplement). As of the latest mortality tracking in 2019, 60% of the sample has died. Almost all deceased respondents (97%) died from internal causes, such as chronic or other unspecified illnesses. Main analyses predict all-cause mortality. Sensitivity analyses replicate our findings excluding deaths from external/unknown causes.

[TABLE 1 HERE]

Covariates. All models include time-invariant and time-varying covariates recorded at respondent and area levels. Time-invariant measures are recorded at Wave 1. Time-varying measures are recorded at all waves. At the respondent level, we include time-invariant measures of *five-year birth cohort* (pre-1905 to 1960+); *race-ethnicity* (non-Hispanic Black, Hispanic, and non-Hispanic White); *sex* (female vs. male); and *educational attainment* (college/postgrad vs. less than college). We exclude Non-Hispanic Native American and Asian respondents due to small cell sizes. Time-varying measures include *marital status* (married vs. not married); *employment status* (employed vs. non-employed/disabled); *family income* (standardized to 1000 USD in 2019); *homeowner status* (owns home vs. does not); and *smoker status* (never vs. current/former smoker). We also include a time-varying indicator for *mover status* (new vs. same residence). At Wave 1, respondents answered whether they had moved to a new place of residence in the last three years. At subsequent waves, respondents answered whether they had moved to a new place of residence since their last interview.

At the area level, we include time-varying measures of *state of residence*, *tract poverty* (proportion of residents below the federal poverty level); *tract rural-urban commuting area (RUCA) codes* (metropolitan vs. small town/rural); and *tract racial clustering*. We employ two tract-level measures of racial segregation that account for the spatial clustering of Black and Hispanic residents using the Getis-Ord i* (Gi*) hotspot Z-score. Scores are categorized as "segregated" (vs. "non-segregated") based on a 1.96 significance threshold.[53] The online supplement includes additional information about the Gi* statistic.

For all tract measures, data originate from the 1990 census for Waves 1 through 3 and the 2000 census for Wave 4. For tract poverty at Waves 5 and 6, data come from American Community Survey (ACS) five-year estimates between 2008-2012 and 2013-2017, respectively. Tract RUCA codes at Waves 5 and 6 originate from the 2010 census. Gi* statistics at Waves 5 and 6 are based on five-year ACS estimates from 2010-2014 and 2015-2019, respectively.

Analysis Plan

Our main models predict survival time in years from birth using fully parametric accelerated failure time (AFT)–shared frailty survival models that account for right censoring, covariates, and multiple observations clustered within respondents. AFT models are distinct from and advantageous over proportional hazards (PH) models in several ways.[54,55] For one, while PH models assume covariates shift the hazard function multiplicatively, AFT models assume covariates accelerate or decelerate the effect of time on survival. The log-linear regression parameters of AFT models are also more robust than PH models to omitted covariates.[55] Shared frailties are cluster-specific random effects for latent common mortality risks ("frailties") of cluster members.[55] In our models, shared frailties account for unobserved heterogeneity and multiple observations clustered within ACL respondents, akin to a random intercept in a multilevel model. Our models assume respondents have unique frailties with mean 1 and finite variance (theta) estimated from the data.

To test this model, we first converted our dataset to long format, resulting in multiple rows per respondent. We then employed the `streg` command in Stata 19 with the `shared` option specified to track respondents' unique study identification numbers across waves.[54] This command performed maximum likelihood estimation for parametric AFT-shared frailty models.

We also tested various model specifications and assumptions for the origin time and survival/frailty distributions. After consulting BIC and likelihood ratio test statistics, we decided on a final model that predicts survival time in years from birth assuming log-logistic survival and gamma frailty distributions. We also tested different functional forms of RSEI toxicity-weighted concentrations. These included: (1) original values; (2) logged values; and (3) linear splines with knots at the median, tertile, quartile, quintile, and decile

points of their distributions. Though fit statistics favored logged values, these proved to be problematic for two reasons. First, logged values resulted in major losses of variance and high correlations ($r > .95$) between buffers, rendering comparisons across RSEI buffers meaningless. Second, logged values assume a linear association between toxicant exposure and mortality. Yet studies cited earlier suggest the effects of air toxicants on mortality are likely non-linear.[4,5] For our main tests, we decided to model RSEI toxicant concentrations as linear splines with tertile knots. To stabilize knots across waves, we constructed splines after converting the dataset to long format. Thus, tertiles should be interpreted relative to the full range of toxicant concentrations observed across the entire ACL study period (1986 to 2019).

We also conducted a series of ancillary analyses. Results for these analyses are tabulated in the online supplement and briefly discussed below. To test the differential vulnerability hypothesis, we modeled interaction terms between toxicity-weighted concentrations and four moderators: (1) respondent race-ethnicity, (2) respondent income, (3) tract racial segregation, and (4) tract poverty. To test the sensitivity of our findings, we also replicated our models in three ways: (1) using logged RSEI concentrations instead of splines; (2) assuming an entry time of Wave 1 with an exponential survival/gamma frailty distribution; and (3) excluding respondents who died of external/undocumented causes.

RESULTS

Sample Characteristics

Table 2 reports descriptive statistics of study variables (excluding state of residence). Means/counts are reported for each variable with standard deviations/percentages in parentheses. Statistics are reported separately for each survey wave. Although recorded only at Wave 1, statistics for time-invariant measures are also included at each wave to document changes in sample composition over time.

The typical ACL respondent at Wave 1 was born around 1932. Most respondents at Wave 1 were also female (63%), non-Hispanic White (61%), married (54%), employed (52%), a homeowner (63%), and living in a metropolitan area (77%). Reviewing toxicity-weighted concentration levels across buffers, average toxicant levels tend to be lowest in the 1- and 2-km buffers, before increasing and leveling off within 5-, 10-,

and 25-km buffers. These patterns are to be expected, given that larger land areas will likely contain more industrial facilities documented in the RSEI-GM database. Depending on respondents' residential locations, however, larger buffers may also include additional bodies of water and/or vacant landmasses that contain little or no recorded air emissions, which could explain why toxicants level off in larger areas.

One striking pattern in Table 2 is the reduction in average air toxicant levels over the study period. For example, average toxicity-weighted concentrations in 25-km buffers plummet from 105,950 to 3,420 between 1986 and 2019. There are at least two explanations for these patterns. First, researchers have found that environmental policies and industrial practices enacted shortly after the start of ACL led to drastic reductions in industrial air emissions nationwide over subsequent decades.[8,9] These include the Community Right to Know Act of 1986, Pollution Prevention Act (PPA) of 1990, and Clean Air Act (CAA) Amendments of 1990. The CAA Amendments, in particular, targeted many of the industrial air toxicants documented in the RSEI-GM database.[56] Second, selective mortality could also be partially responsible. That is, respondents who were socioeconomically disadvantaged in early waves could have been both more likely to live in heavily polluted areas and to die prematurely, which may have further contributed to observed declines in average pollution levels over the study period. For instance, we also observe changes in the ACL sample composition across Waves 1 to 6, such that surviving respondents have become increasingly college educated (13% to 28%), higher income ($64k to $89k in 2019 USD), and White (61% to 70%); more respondents also report being homeowners (63% to 80%) and residing in tracts with lower poverty rates (18% to 14%).

[TABLE 2 HERE]

Survival Model Results

Table 3 reports results from multivariable AFT-shared frailty models. Results are reported as exponentiated survival time ratios (TR) with 95% confidence intervals (CIs) in brackets. TRs less/greater than 1.00 indicate shorter/longer survival times. Accompanying Table 3 is a set of graphs depicting marginal predicted survival times as a function of RSEI toxicity-weighted concentration splines across all spatial buffers (Figure 1).

Table 3 reveals significant non-linear associations between toxicity-weighted concentrations and survival. Due to their wide scales, TRs for toxicity-weighted concentration splines are difficult to interpret. Generally, we find that increases in toxicity-weighted concentrations within the first two splines predict shorter survival times across all buffers, holding covariates constant. For 25-km buffers only, we also observe an additional decline in survival between the second and third spline of toxicity-weighted concentrations.

[TABLE 3 HERE]

Figure 1 clarifies these associations. For each graph, the x-axis depicts tertile knots for the RSEI toxicity-weighted concentration splines. The y-axis represents predicted survival time in years from birth. For 1-km and 2-km buffers, we observe one-year declines in survival time within the first and second splines, but no additional declines within the third spline. The result is a two-year total gap in survival time between respondents who reside in areas with the highest (100%) versus lowest (0%) toxicant concentrations (~73.5 vs. ~ 75.5 years). We begin to observe additional declines in survival within the third splines of 5-, 10-, and 25-km buffers. For example, we observe a four-year total gap in survival between respondents living in 25-km buffers with the highest (100%) versus lowest (0%) toxicant concentrations (~71.5 vs. ~75.5 years).

[FIGURE 1 HERE]

We also find some evidence of differential vulnerability. The full set of tests is tabulated in the online supplement (Tables S1-S5). Here, we focus only on a handful of significant interactions from these tables, which we graph in Figures 2 and 3. First, Model 5 of Table S1 shows that the inverse association between survival time and toxicant concentration splines recorded within 5-km buffers is significantly larger for Black (vs. White) respondents, particularly in buffers with concentrations recorded within the highest tertile spline. This non-linear interaction is graphed in Figure 2. This figure shows that for White respondents, the total gap in survival time between respondents who reside in 5-km buffers with the highest (100%) versus lowest (0%) toxicant concentrations is around two years (~74 vs. ~76 years). However, for Black respondents, this same gap is nearly 12 years (~62 vs. ~74 years), with roughly 9 years of this total gap observed among Black respondents living in areas with toxicant concentrations recorded within the third tertile.

[FIGURE 2 HERE]

Second, Model 9 in Tables S2 and S3, respectively, show that the inverse associations between survival and RSEI toxicity-weighted concentration splines recorded in 25-km buffers are buffered for respondents who report higher incomes, and exacerbated for respondents who live in census tracts with higher poverty rates. Figure 3 graphs these non-linear interactions by respondent incomes (top) and tract poverty rates (bottom). Although our interaction terms treated income and poverty as continuous variables, we split the graphs into "high" (top 10%) and "low" (bottom 25%) income and poverty groups for the sake of visual demonstration. Relative to their peers who report high incomes or reside in low-poverty tracts, respectively, those with low incomes and who reside in high-poverty tracts exhibit steeper declines in survival when residing in 25-km buffers with toxicant levels recorded within the third tertile.

There were three additional significant interactions we did not graph. First, Models 8 and 10 in Table S1 reveal similar interactions with respondent race-ethnicity (Black vs. White) when testing logged toxicant concentrations within 10- and 25-km spatial buffers. Second, Model 7 of Table S2 also indicates a similar moderation pattern by respondent incomes when modeling toxicant concentration splines within 10-km buffers. Finally, Tables S4 and S5 provide no evidence of moderation by tract racial segregation.

[FIGURE 3 HERE]

Sensitivity Analyses

Sensitivity analyses are tabulated in the online supplement and briefly discussed here. First, Stata currently does not support probability weighting with shared frailty models. Thus, our main results are unweighted. To confirm that weighting does not alter our main findings, we replicated our main results with and without weights using respondent-level clustered standard errors instead of shared frailties (Table S6). Second, logged toxicity-weighted concentrations produce similar results, albeit at the expense of informative variance across spatial buffers (Figure S2). Third, we observe comparable patterns when assuming an entry time of Wave 1 with exponential survival and gamma frailty distributions (Table S7; Figures S3 and S4). Fourth, results are identical excluding 53 respondents who died from external or unknown causes (Table S8).

DISCUSSION

We uncovered three key findings. First, consistent with prior work,[4,5] we found non-linear associations between measures of industrial air toxicant concentrations and individual mortality, such that adults who lived in areas with relatively low toxicant concentrations still tended to die 1-2 years earlier than peers who lived in areas with few or no toxicants. Second, the magnitude of associations between toxicant concentrations and mortality varied depending on the size of the exposure area. Within smaller areas approximating the size of neighborhoods, associations between toxicant concentrations and mortality leveled off at high toxicant levels, resulting in a 2-year total mortality gap between respondents living in the most versus least polluted areas. However, when considering toxicant concentrations within larger areas approximating the size of cities, we found a 4-year total mortality gap between respondents living in the most versus least polluted areas. Third, several of these associations were amplified for respondents who reported lower incomes, identified as non-Hispanic Black (vs. White), or resided in high-poverty census tracts.

Our study is characterized by limitations common to cohort studies in this area.[3] First, RSEI-GM data are indirect proxies of exposure to industrial air toxicants, and thus should not be considered direct measures of exposure. Second, RSEI-GM only accounts for emissions from certain industry sectors who are legally mandated to report to TRI. Other important sources of air pollution to consider in future research are biogenic sources (e.g., wildfires), and emissions from transportation and residential sectors, to name a few.[1] Third, our censored survival models do not account for underlying biological pathways or disease initiation and progression, and thus provide little insight into nonfatal health conditions linked to toxicant exposure. On a similar note, because ACL originally sampled adults ages 25 to 96, our models cannot account for toxicant exposures during critical or sensitive developmental periods earlier in the life course.[57] Finally, although our models accounted for various sources of confounding at individual and spatial levels, our mortality estimates are based on observational data and still could be biased by omitted covariates. For example, unmeasured hazardous workplace exposures may at least partially explain some of our findings, especially results observed among Black and lower-income respondents.[58,59]

Despite these limitations, our findings have critical implications for researchers and policymakers. For the research community, we are among the first to link RSEI-GM indicators with individual mortality data from a large and nationally representative longitudinal cohort. By accounting for non-linear associations across multiple spatial buffers, we also uncovered evidence to suggest distinct mechanisms linking individual mortality risk with industrial air toxicant exposures over the adult life course. For instance, we found the largest toxicant-mortality associations within 25-km buffers. This suggests measures of industrial air toxicants recorded in larger land areas may gauge a broader swath of exposures encompassing daily activity spaces beyond residential locations, including workplaces, commuting routes, and other recreational spaces.[60,61]

We also provide a novel test of the differential vulnerability hypothesis. Recall that this hypothesis suggests industrial air toxicant exposure will be more harmful for the health of otherwise vulnerable or distressed groups.[16–18] Our analyses uncovered evidence of differential vulnerability among respondents who reported lower incomes, identified as non-Hispanic Black, or resided in high-poverty tracts, specifically when modeling high industrial air toxicant levels within larger spatial buffers approximating the size of cities. There are at least two plausible explanations for these patterns. First, disadvantaged groups may experience other chronic stressors that interact with and compound the adverse health effects of air toxicants, including financial strain, unfair treatment, and exposure to neighborhood violence and disorder.[22,23,49] Second, compared to their White and affluent peers, the daily commutes and routines of disadvantaged populations may be geographically isolated to other polluted locations beyond their residential contexts. For example, activity space studies have found that residents tend to visit other locations within their cities that have similar socioeconomic compositions as their residential contexts.[62] This may explain why we only found evidence of differential vulnerability when modeling industrial air toxicants within larger spatial buffers.

Our findings have three key policy takeaways. First, consistent with past studies,[4,5] our results suggest that even low levels of air toxicant exposure can accumulate within the body over time to gradually accelerate mortality. Second, interventions designed to mitigate the dangers of industrial air toxicants to human health should consider multiscalar approaches, incorporating mitigation strategies at multiple geographic levels. Though neighborhood scales are important, our results also suggest interventions targeting air toxicants

within broader administrative areas like cities or counties may be most effective at reducing population-level mortality disparities. This finding can inform EPA regulators concerned with developing updated health-protective standards and "residual risk rules" under the 1990 CAA Amendments.[63] Third, we found evidence to suggest that the most lethal levels of industrial air toxicants were recorded prior to major federal air pollution regulations of the 1990s, which led to drastic reductions in industrial emissions nationwide over subsequent decades (e.g., PPA and CAA Amendments of 1990). These findings indicate that any attempts to roll back or eliminate environmental regulations could have dire consequences for US life expectancy.

REFERENCES

1. Thakrar SK, Balasubramanian S, Adams PJ, et al. Reducing Mortality from Air Pollution in the United States by Targeting Specific Emission Sources. *Environ Sci Technol Lett*. 2020;7(9):639-645. doi:10.1021/acs.estlett.0c00424

2. Burnett R, Chen H, Szyszkowicz M, et al. Global estimates of mortality associated with long-term exposure to outdoor fine particulate matter. *Proc Natl Acad Sci USA*. 2018;115(38):9592-9597. doi:10.1073/pnas.1803222115

3. Pope CA, Coleman N, Pond ZA, Burnett RT. Fine particulate air pollution and human mortality: 25+ years of cohort studies. *Environmental Research*. 2020;183:108924. doi:10.1016/j.envres.2019.108924

4. Weichenthal S, Pinault L, Christidis T, et al. How low can you go? Air pollution affects mortality at very low levels. *Sci Adv*. 2022;8(39):eabo3381. doi:10.1126/sciadv.abo3381

5. Shi L, Rosenberg A, Wang Y, et al. Low-Concentration Air Pollution and Mortality in American Older Adults: A National Cohort Analysis (2001–2017). *Environ Sci Technol*. 2022;56(11):7194-7202. doi:10.1021/acs.est.1c03653

6. House JS. Americans' Changing Lives: Waves I and II, 1986 and 1989. Published online 1986.

7. Hicken M. Americans' Changing Lives: Wave VI. Published online 2019.

8. Zhang Y, West JJ, Mathur R, et al. Long-term trends in the ambient PM2.5- and O3-related mortality burdens in the United States under emission reductions from 1990 to 2010. *Atmos Chem Phys*. 2018;18(20):15003-15016. doi:10.5194/acp-18-15003-2018

9. LaCount MD, Haeuber RA, Macy TR, Murray BA. Reducing power sector emissions under the 1990 Clean Air Act Amendments: A retrospective on 30 years of program development and implementation. *Atmospheric Environment*. 2021;245:118012. doi:10.1016/j.atmosenv.2020.118012

10. Environmental Protection Agency. *EPA's Risk-Screening Environmental Indicators (RSEI) Methodology: RSEI Version 2.3.8*. Office of Pollution Prevention and Toxics.

11. Mohai P, Kweon BS, Lee S, Ard K. Air Pollution Around Schools Is Linked To Poorer Student Health And Academic Performance. *Health Affairs*. 2011;30(5):852-862. doi:10.1377/hlthaff.2011.0077

12. Ard K. Trends in exposure to industrial air toxins for different racial and socioeconomic groups: A spatial and temporal examination of environmental inequality in the U.S. from 1995 to 2004. *Social Science Research*. 2015;53:375-390. doi:10.1016/j.ssresearch.2015.06.019

13. Ard K, Thomas J, Bullock C. Toxic air pollution and cognitive decline: Untangling particulate matter. *Health & Place*. 2024;89:103330. doi:10.1016/j.healthplace.2024.103330

14. Priem B, Wodtke GT, Ard K. Racial Disparities in Childhood Exposure to Neurotoxic Air Pollution. *Journal of Health and Social Behavior*. 2025;Online first. doi:doi.org/10.1177/00221465251340064

15. Crane BM, Moored KD, Donahue PT, et al. Associations between toxicity-weighted concentrations and dementia risk: Results from the Cardiovascular Health Cognition Study. *Science of The Total Environment*. 2024;945:173706. doi:10.1016/j.scitotenv.2024.173706

16. Hicken MT, Adar SD, Hajat A, et al. Air Pollution, Cardiovascular Outcomes, and Social Disadvantage: The Multi-ethnic Study of Atherosclerosis. *Epidemiology*. 2016;27(1):42-50. doi:10.1097/ede.0000000000000367

17. Hicken MT, Adar SD, Diez Roux AV, et al. Do Psychosocial Stress and Social Disadvantage Modify the Association Between Air Pollution and Blood Pressure?: The Multi-Ethnic Study of Atherosclerosis. *American Journal of Epidemiology*. 2013;178(10):1550-1562. doi:10.1093/aje/kwt190

18. Hicken MT, Dvonch JT, Schulz AJ, Mentz G, Max P. Fine particulate matter air pollution and blood pressure: The modifying role of psychosocial stress. *Environmental Research*. 2014;133:195-203. doi:10.1016/j.envres.2014.06.001

19. Turner RJ. Understanding Health Disparities: The Relevance of the Stress Process Model. *Society and Mental Health*. 2013;3(3):170-186. doi:10.1177/2156869313488121

20. Clouston SAP, Link BG. A Retrospective on Fundamental Cause Theory: State of the Literature and Goals for the Future. *Annual Review of Sociology*. 2021;47:1-26.

21. Boen CE, Yang YC, Aiello AE, et al. Patterns and Life Course Determinants of Black–White Disparities in Biological Age Acceleration: A Decomposition Analysis. *Demography*. 2023;60(6):1815-1841. doi:10.1215/00703370-11057546

22. Brown TH, Hargrove TW, Homan P, Adkins DE. Racialized Health Inequities: Quantifying Socioeconomic and Stress Pathways Using Moderated Mediation. *Demography*. 2023;60(3):675-705. doi:10.1215/00703370-10740718

23. Hicken MT, Lee H, Ailshire J, Burgard SA, Williams DR. "Every Shut Eye, Ain't Sleep": The Role of Racism-Related Vigilance in Racial/Ethnic Disparities in Sleep Difficulty. *Race and Social Problems*. 2013;5(2):100-112. doi:10.1007/s12552-013-9095-9

24. DeAngelis RT. Striving While Black: Race and the Psychophysiology of Goal Pursuit. *J Health Soc Behav*. 2020;61(1):24-42. doi:10.1177/0022146520901695

25. Boen CE, Hummer RA. Longer—but Harder—Lives?: The Hispanic Health Paradox and the Social Determinants of Racial, Ethnic, and Immigrant–Native Health Disparities from Midlife through Late Life. *J Health Soc Behav*. 2019;60(4):434-452. doi:10.1177/0022146519884538

26. DeAngelis RT. Moving on Up? Neighborhood Status and Racism-Related Distress among Black Americans. *Social Forces*. 2022;100(4):1503-1532. doi:https://doi.org/10.1093/sf/soab075

27. DeAngelis RT, Hargrove TW, Hummer RA. Skin Tone and the Health Returns to Higher Status. *Demography*. 2022;59(5):1791-1819. doi:10.1215/00703370-10191675

28. Boen C. The role of socioeconomic factors in Black-White health inequities across the life course: Point-in-time measures, long-term exposures, and differential health returns. *Social Science & Medicine*. 2016;170:63-76. doi:10.1016/j.socscimed.2016.10.008

29. Assari S. Health disparities due to diminished return among black Americans: Public policy solutions. *Social Issues and Policy Review*. 2018;12(1):112-145.

30. Colen CG, Ramey DM, Cooksey EC, Williams DR. Racial disparities in health among nonpoor African Americans and Hispanics: The role of acute and chronic discrimination. *Social Science & Medicine*. 2018;199:167-180. doi:10.1016/j.socscimed.2017.04.051

31. Massey DS. Still the Linchpin: Segregation and Stratification in the USA. *Race Soc Probl*. 2020;12(1):1-12. doi:10.1007/s12552-019-09280-1

32. Chen L, Mitchell BC, Laurent SE, Edlebi JK, Meier HCS. Historical redlining and contemporary home mortgage lending: Investigating neighborhood-level racial disparities in mortgage originations in the United States. *Cities*. 2026;170:106632. doi:10.1016/j.cities.2025.106632

33. Schieman S. Residential Stability and the Social Impact of Neighborhood Disadvantage: A Study of Gender- and Race-Contingent Effects. *Social Forces*. 2005;83(3):1031-1064. doi:10.1353/sof.2005.0045

34. York Cornwell E, Goldman AW. Neighborhood Disorder and Distress in Real Time: Evidence from a Smartphone-Based Study of Older Adults. *J Health Soc Behav*. 2020;61(4):523-541. doi:10.1177/0022146520967660

35. Gruber A. Policing and "Bluelining." *Houston Law Review*. 2021;58:867-936.

36. Hanna-Attisha M, LaChance J, Sadler RC, Champney Schnepp A. Elevated Blood Lead Levels in Children Associated With the Flint Drinking Water Crisis: A Spatial Analysis of Risk and Public Health Response. *Am J Public Health*. 2016;106(2):283-290. doi:10.2105/AJPH.2015.303003

37. Aelion CM, Davis HT, Lawson AB, Cai B, McDermott S. Associations between soil lead concentrations and populations by race/ethnicity and income-to-poverty ratio in urban and rural areas. *Environ Geochem Health*. 2013;35(1):1-12. doi:10.1007/s10653-012-9472-0

38. Cooksey-Stowers K, Schwartz MB, Brownell KD. Food Swamps Predict Obesity Rates Better Than Food Deserts in the United States. *International Journal of Environmental Research and Public Health*. 2017;14(11):11. doi:10.3390/ijerph14111366

39. Kong AY, Lee JGL, Halvorson-Fried SM, et al. Neighbourhood inequities in the availability of retailers selling tobacco products: a systematic review. *Tob Control*. Published online June 27, 2024:tc-2024-058718. doi:10.1136/tc-2024-058718

40. Nardone A, Rudolph KE, Morello-Frosch R, Casey JA. Redlines and Greenspace: The Relationship between Historical Redlining and 2010 Greenspace across the United States. *Environ Health Perspect*. 2021;129(1):017006. doi:10.1289/EHP7495

41. Massey DS, Wagner B. Segregation, Stigma, and Stratification: A Biosocial Model. In: Major B, Dovidio JF, Link BG, eds. *The Oxford Handbook of Stigma, Discrimination, and Health*. Vol 1. Oxford University Press; 2017:147-162. doi:10.1093/oxfordhb/9780190243470.013.14

42. Mayne SL, Hicken MT, Merkin SS, et al. Neighbourhood racial/ethnic residential segregation and cardiometabolic risk: the multiethnic study of atherosclerosis. *J Epidemiol Community Health*. 2019;73(1):26-33. doi:10.1136/jech-2018-211159

43. Kershaw KN, Robinson WR, Gordon-Larsen P, et al. Association of Changes in Neighborhood-Level Racial Residential Segregation With Changes in Blood Pressure Among Black Adults: The CARDIA Study. *JAMA Intern Med*. 2017;177(7):996. doi:10.1001/jamainternmed.2017.1226

44. Hicken MT, Payne-Sturges D, McCoy E. Evaluating Race in Air Pollution and Health Research: Race, PM2.5 Air Pollution Exposure, and Mortality as a Case Study. *Curr Envir Health Rpt*. 2023;10(1):1-11. doi:10.1007/s40572-023-00390-y

45. Laurent O, Bard D, Filleul L, Segala C. Effect of socioeconomic status on the relationship between atmospheric pollution and mortality. *Journal of Epidemiology & Community Health*. 2007;61(8):665-675. doi:10.1136/jech.2006.053611

46. Josey KP, Delaney SW, Wu X, et al. Air Pollution and Mortality at the Intersection of Race and Social Class. *N Engl J Med*. 2023;388(15):1396-1404. doi:10.1056/NEJMsa2300523

47. Jorgenson AK, Hill TD, Clark B, et al. Power, proximity, and physiology: does income inequality and racial composition amplify the impacts of air pollution on life expectancy in the United States? *Environ Res Lett*. 2020;15(2):024013. doi:10.1088/1748-9326/ab6789

48. Hill TD, Jorgenson AK, Ore P, Balistreri KS, Clark B. Air quality and life expectancy in the United States: An analysis of the moderating effect of income inequality. *SSM - Population Health*. 2019;7:100346. doi:10.1016/j.ssmph.2018.100346

49. DeAngelis RT. Racial Capitalism and Black–White Health Inequities in the United States: The Case of the 2008 Financial Crisis. *J Health Soc Behav*. 2025;66(2):148-164. doi:10.1177/00221465241260103

50. Mohai P, Lantz PM, Morenoff J, House JS, Mero RP. Racial and Socioeconomic Disparities in Residential Proximity to Polluting Industrial Facilities: Evidence From the Americans' Changing Lives Study. *Am J Public Health*. 2009;99(S3):S649-S656. doi:10.2105/ajph.2007.131383

51. US EPA. *RSEI Toxicity-Data and Calculations*. US Environmental Protection Agency; 2025. https://www.epa.gov/rsei/rsei-toxicity-data-and-calculations

52. US EPA. *National Air Quality and Emissions Trends Report, 1989*. US Environmental Protection Agency; 1991.

53. Kershaw KN, Robinson WR, Gordon-Larsen P, et al. Association of Changes in Neighborhood-Level Racial Residential Segregation With Changes in Blood Pressure Among Black Adults: The CARDIA Study. *JAMA Intern Med*. 2017;177(7):996. doi:10.1001/jamainternmed.2017.1226

54. Gutierrez RG. Parametric Frailty and Shared Frailty Survival Models. *The Stata Journal: Promoting communications on statistics and Stata*. 2002;2(1):22-44. doi:10.1177/1536867X0200200102

55. Gorfine M, Zucker DM. Shared Frailty Methods for Complex Survival Data: A Review of Recent Advances. *Annu Rev Stat Appl*. 2023;10(1):51-73. doi:10.1146/annurev-statistics-032921-021310

56. United States Environmental Protection Agency. 1990 Clean Air Act Amendment Summary: Title III. 2024. Accessed July 28, 2025. https://www.epa.gov/clean-air-act-overview/1990-clean-air-act-amendment-summary-title-iii

57. Kuh D, Ben-Shlomo Y, Lynch J, Hallqvist J, Power C. Life course epidemiology. *Journal of Epidemiology & Community Health*. 2003;57(10):778-783. doi:10.1136/jech.57.10.778

58. Jalasto J, Luukkonen R, Lindqvist A, et al. Occupational exposure to vapors, gasses, dusts, and fumes in relation to causes of death during 24 years in Helsinki, Finland. *Int Arch Occup Environ Health*. 2024;97(2):145-154. doi:10.1007/s00420-023-02031-1

59. Viel JF, Bonvallot N, Dab W. Integration of Occupational Exposure into the Exposome. In: *Handbook of Life Course Occupational Health*. Springer, Cham; 2023:1-16. doi:10.1007/978-3-030-94023-2_7-1

60. Finlay J, Esposito M, Kim MH, Gomez-Lopez I, Clarke P. Closure of 'third places'? Exploring potential consequences for collective health and wellbeing. *Health & Place*. 2019;60:102225. doi:10.1016/j.healthplace.2019.102225

61. Cagney KA, York Cornwell E, Goldman AW, Cai L. Urban Mobility and Activity Space. *Annu Rev Sociol*. 2020;46(1):623-648. doi:10.1146/annurev-soc-121919-054848

62. Cai L, Browning CR, Cagney KA. Exposure of Neighborhood Racial and Socio-Economic Composition in Activity Space: A New Approach Adjusting for Residential Conditions. *Social Forces*. 2024;103(1):350-373. doi:10.1093/sf/soae021

63. United States Environmental Protection Agency. Risk and Technology Review of the National Emissions Standards for Hazardous Air Pollutants. 2025. Accessed July 28, 2025. https://www.epa.gov/stationary-sources-air-pollution/risk-and-technology-review-national-emissions-standards-hazardous

TABLES AND FIGURES

Table 1. Description of Survival Data: Americans' Changing Lives, Wave 6 (2019; N = 3,329).

	Total	Mean	Median	Min.	Max.
Respondents	3,329	—	—	—	—
Recorded deaths	1,994	—	—	—	—
Survival time from birth (years)	254,297.42	76.39	76.75	26.58	115.17
Survival time from Wave 1 (years)	74,751.17	22.45	25.08	0.08	33.58
Causes of death					
Cancer	398	0.20	—	—	—
Diabetes	71	0.04	—	—	—
Cardiovascular	637	0.32	—	—	—
Cerebrovascular	197	0.10	—	—	—
Neurodegenerative	117	0.06	—	—	—
Other disease	521	0.26	—	—	—
External cause	13	0.01	—	—	—
Undocumented	40	0.02	—	—	—

Note: For causes of death, the mean column represents the proportion of respondents who died from each cause.

Table 2. Descriptive Statistics of Study Variables: Americans' Changing Lives, Waves 1-6 (1986-2019).

	Wave 1 (1986)		Wave 2 (1989)		Wave 3 (1994)	
RSEI toxicity-weighted concentrations [a, c]						
1-km buffer	72,336.69	(427,365.42)	64,060.12	(351,934.49)	16,685.27	(90,341.59)
2-km buffer	95,119.14	(397,616.77)	87,566.05	(353,753.45)	22,729.16	(86,029.66)
5-km buffer	108,889.20	(288,226.35)	104,555.71	(280,222.88)	29,680.47	(104,530.74)
10-km buffer	107,249.14	(212,638.32)	105,194.18	(249,817.55)	30,411.17	(75,302.46)
25-km buffer	105,367.03	(181,322.22)	100,665.57	(188,736.73)	27,680.04	(54,393.87)
Birth year [b]	1932.12	(17.59)	1932.73	(17.06)	1934.35	(16.54)
Race-ethnicity [b]						
Non-Hispanic Black	1,108	(33%)	819	(31%)	684	(29%)
Hispanic	182	(5%)	129	(5%)	112	(5%)
Non-Hispanic White	2,039	(61%)	1,662	(64%)	1,526	(66%)
Female (vs. male) [b]	2,081	(63%)	1,667	(64%)	1,483	(64%)
College degree (vs. less) [b]	443	(13%)	384	(15%)	363	(16%)
Married (vs. not) [a]	1,783	(54%)	1,417	(54%)	1,268	(55%)
Employed (vs. non-employed/disabled) [a]	1,723	(52%)	1,344	(51%)	1,127	(49%)
Family income (1000 USD in 2019) [a]	63.65	(42.87)	65.71	(42.96)	64.23	(42.42)
Homeowner (vs. not) [a]	2,113	(63%)	1,796	(69%)	1,670	(72%)
Never smoked (vs. current/former smoker) [a]	1,471	(44%)	1,167	(45%)	1,042	(45%)
Recently moved (vs. same residence) [a]	851	(26%)	600	(23%)	634	(27%)
Tract poverty rate [a]	.18	(.15)	.17	(.14)	.15	(.14)
Segregated Black tract (vs. not) [a]	837	(25%)	589	(23%)	474	(20%)
Segregated Hispanic tract (vs. not) [a]	376	(11%)	260	(10%)	203	(9%)
Metro area (vs. small town/rural) [a]	2,566	(77%)	2,003	(77%)	1,798	(77%)
Total N	3,329		2,610		2,322	

Note: Means/counts are reported with standard deviations/percentages in parentheses.

[a] Time-varying measure recorded at each wave.

[b] Time-invariant measure recorded at Wave 1.

[c] Toxicity-weighted concentrations quantify industrial air toxicant emissions weighted by each toxicant's known potential to cause chronic human health conditions. Concentrations are recorded within five increasing spatial buffers (1-km to 25-km) encircling respondents' residential addresses at each wave.

Table 2. Continued.

	Wave 4 (2001-2)		Wave 5 (2011)		Wave 6 (2019)	
RSEI toxicity-weighted concentrations [a, c]						
1-km buffer	5,683.91	(27,243.72)	2,994.35	(14,018.68)	1,669.47	(7,597.18)
2-km buffer	8,371.93	(31,293.55)	4,851.87	(21,998.04)	2,341.27	(8,381.84)
5-km buffer	11,825.66	(36,174.48)	6,811.45	(33,429.61)	3,593.46	(16,425.15)
10-km buffer	12,006.26	(23,354.49)	8,927.59	(58,061.35)	4,072.62	(19,303.17)
25-km buffer	10,562.56	(15,578.72)	7,549.25	(31,041.37)	3,331.61	(10,779.65)
Birth year [b]	1938.46	(14.97)	1944.51	(12.23)	1948.53	(8.60)
Race-ethnicity [b]						
Non-Hispanic Black	328	(26%)	376	(29%)	154	(24%)
Hispanic	54	(4%)	77	(6%)	38	(6%)
Non-Hispanic White	874	(70%)	839	(65%)	438	(70%)
Female (vs. male) [b]	785	(63%)	805	(62%)	373	(59%)
College degree (vs. less) [b]	229	(18%)	268	(21%)	176	(28%)
Married (vs. not) [a]	699	(56%)	662	(51%)	350	(56%)
Employed (vs. non-employed/disabled) [a]	614	(49%)	547	(42%)	222	(35%)
Family income (1000 USD in 2019) [a]	70.45	(42.40)	95.29	(76.79)	88.58	(66.51)
Homeowner (vs. not) [a]	968	(77%)	918	(71%)	503	(80%)
Never smoked (vs. current/former smoker) [a]	580	(46%)	568	(44%)	282	(45%)
Recently moved (vs. same residence) [a]	408	(32%)	572	(44%)	373	(59%)
Tract poverty rate [a]	.13	(.11)	.16	(.12)	.14	(.11)
Segregated Black tract (vs. not) [a]	246	(20%)	231	(18%)	112	(18%)
Segregated Hispanic tract (vs. not) [a]	119	(9%)	134	(10%)	48	(8%)
Metro area (vs. small town/rural) [a]	1,043	(83%)	1,096	(85%)	537	(85%)
Total N	1,256		1,292		630	

Note: Means/counts are reported with standard deviations/percentages in parentheses.

[a] Time-varying measure recorded at each wave.

[b] Time-invariant measure recorded at Wave 1.

[c] Toxicity-weighted concentrations quantify industrial air toxicant emissions weighted by each toxicant's known potential to cause chronic human health conditions. Concentrations are recorded within five increasing spatial buffers (1-km to 25-km) encircling respondents' residential addresses at each wave.

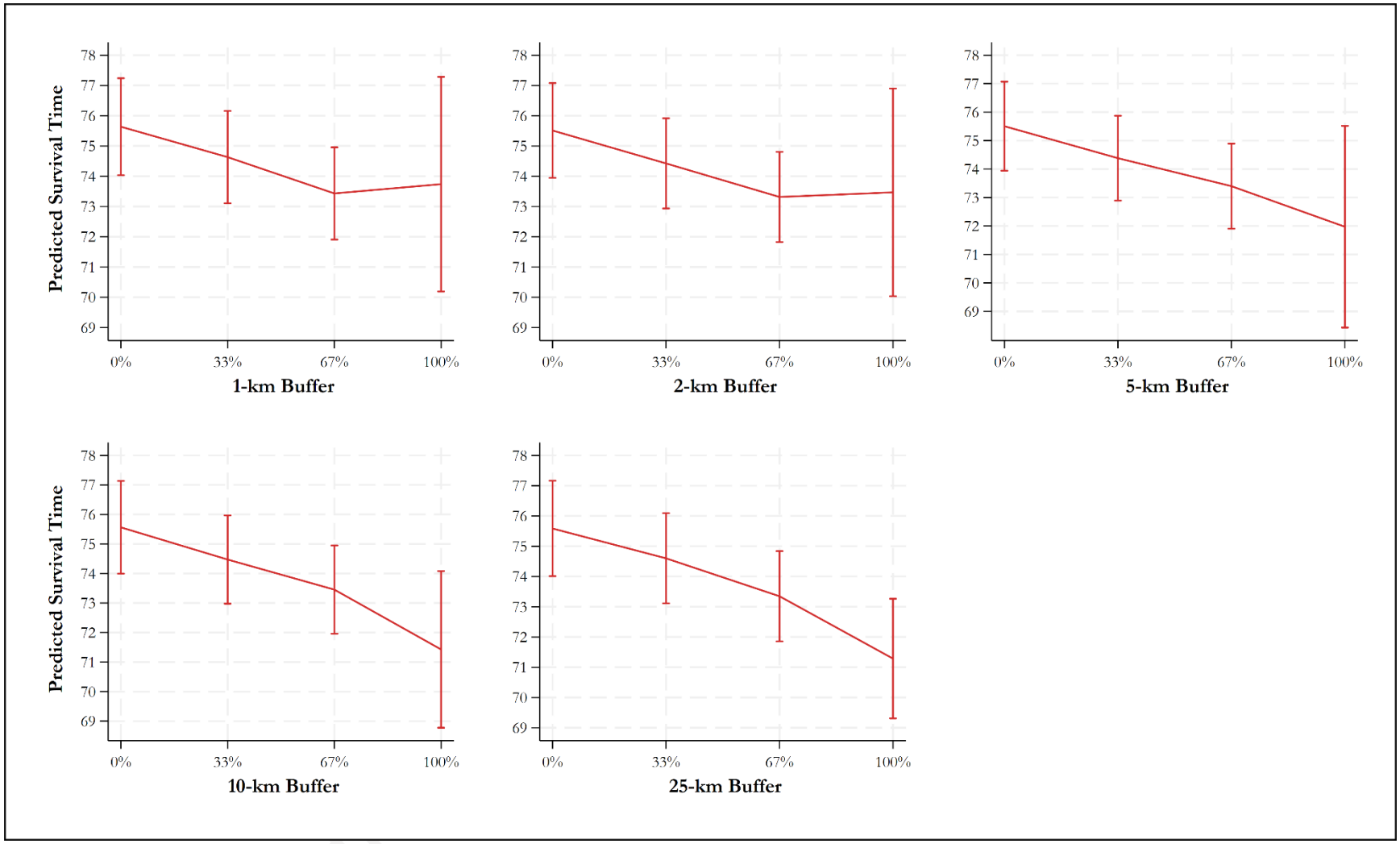

Figure 1. Predicted Survival Time from Birth by RSEI Toxicity-Weighted Concentration Splines: ACL Study, 1986-2019 (N = 3,329).

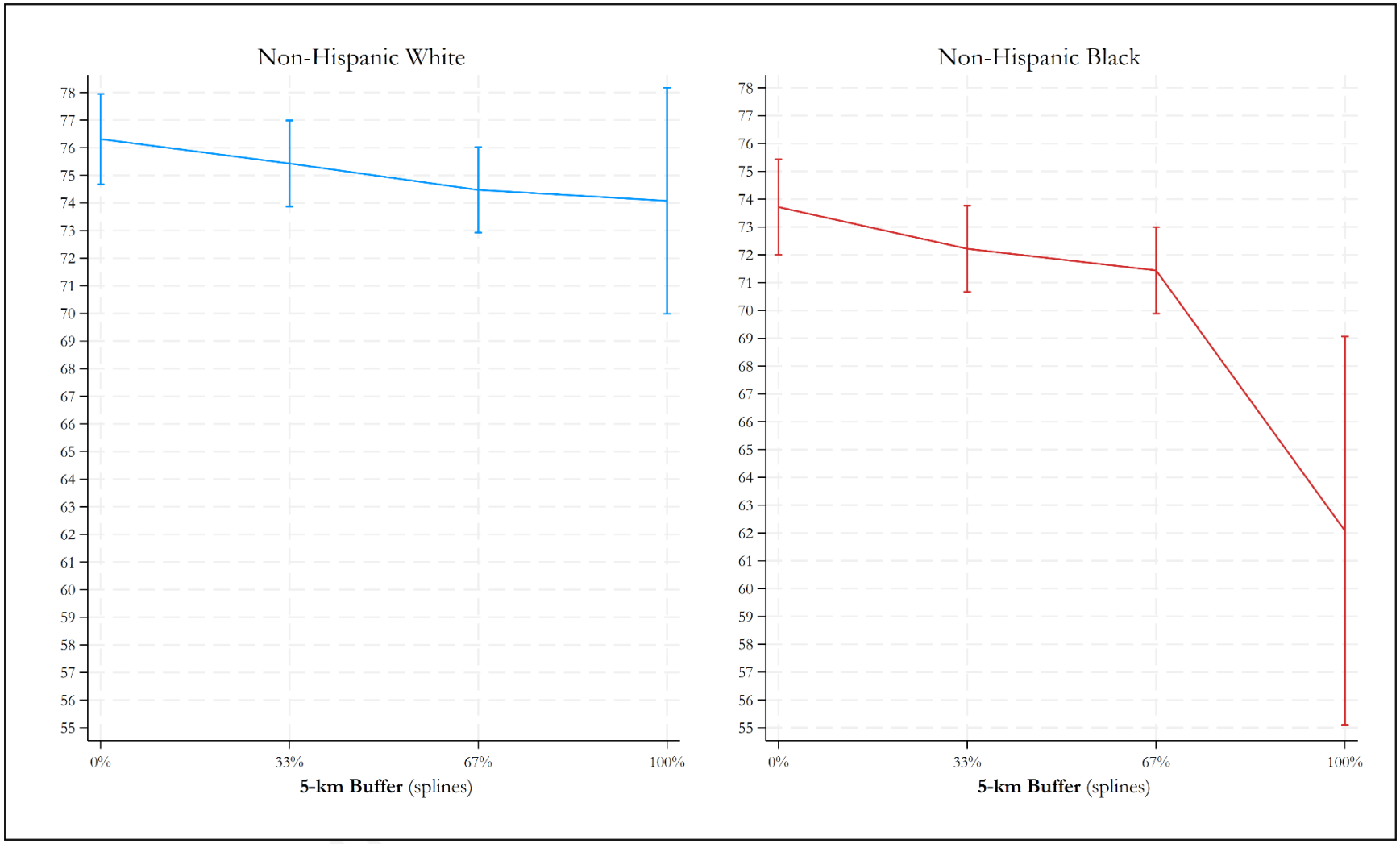

Figure 2. Predicted Survival Time from Birth by 5-km RSEI Toxicity-Weighted Concentration Splines and Respondent Race-Ethnicity: ACL Study, 1986-2019 (N = 3,329).

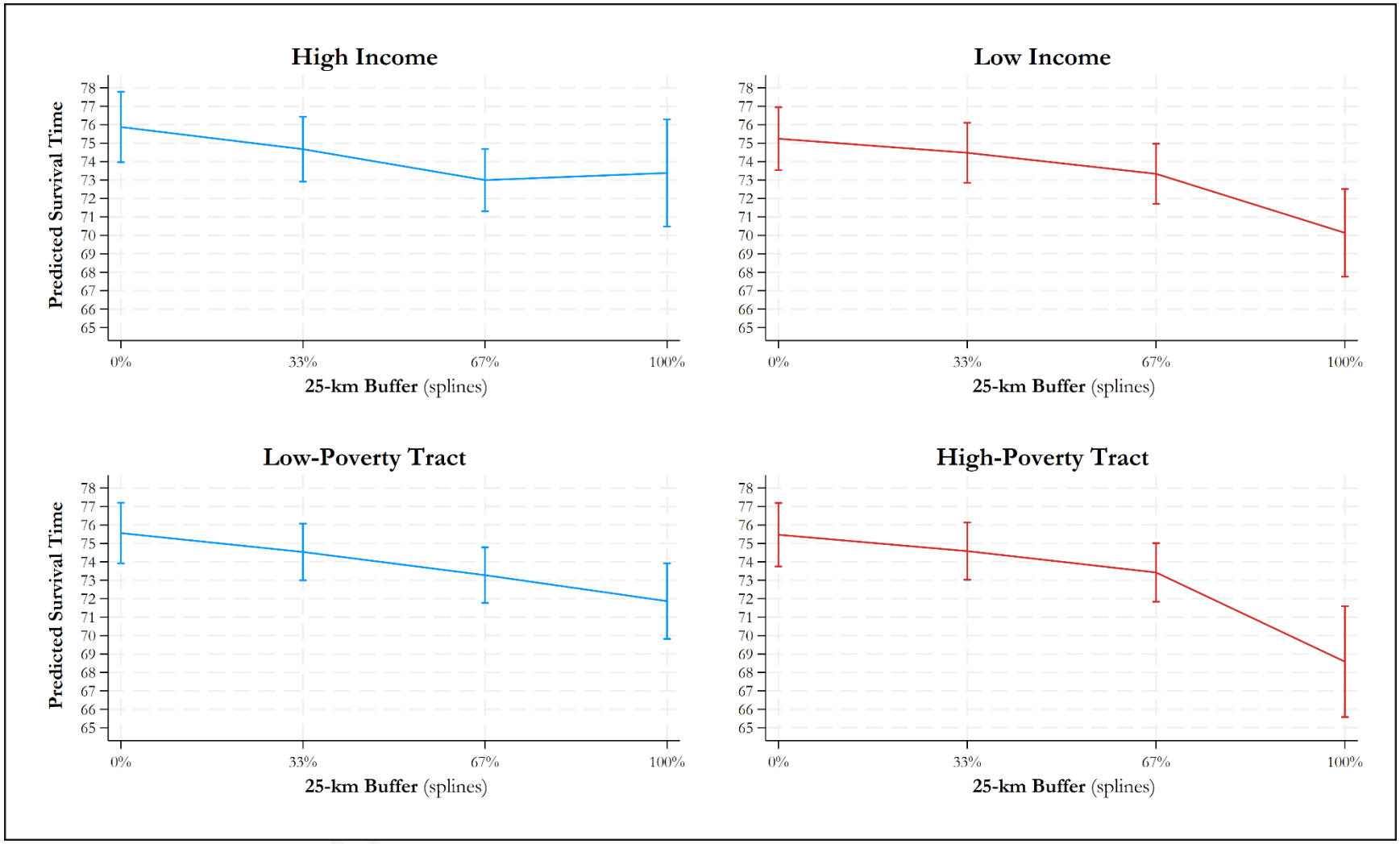

Figure 3. Predicted Survival Time from Birth by 25-km RSEI Toxicity-Weighted Concentration Splines and Respondent Income (top panel) and Tract Poverty (bottom panel): ACL Study, 1986-2019 (N = 3,329).

ONLINE SUPPLEMENT

Getis-Ord (Gi*) Statistic

The Gi* statistic returns a Z-score for each tract, reflecting the extent to which the proportion of Black/Hispanic residents in the tract deviates from the expected proportion of Black/Hispanic residents in the broader census-based statistical area (CBSA) or county in which the tract is located.[1] The Gi* statistics used in our analyses are queen contiguity scores that further weight the composition of the focal tract by all neighboring tracts sharing a common vertex (i.e., edge or corner). To identify segregated and non-segregated tracts, we dichotomize Z-scores using a 1.96 significance threshold, whereby tracts that score at or above 1.96 are classified as "segregated" and those that score below 1.96 are considered "non-segregated." [2]

We measure tract-level segregation with Gi* statistics for several reasons. First, contrary to county- or metro-level (a.k.a., "global") segregation measures, the Gi* statistic is a local neighborhood measure of segregation.[3] Local segregation measures are more relevant for the differential vulnerability hypothesis, which is concerned with residential contexts as moderators of the health effects of air pollution. Second, tract-level Gi* statistics incorporate queen contiguity weights to account for spatial clustering of similar neighboring tracts, thereby proxying broader legacies of concentrated racialized (dis)investment within a CBSA or county. Third, while other commonly used local segregation measures also account for spatial clustering of tracts, the Gi* statistic further accounts for between-CBSA/county patterns of segregation, which is necessary for a national study like ours.[4] For example, this feature accounts for the fact that Black residential segregation will mean something quite different in cities like Seattle, Washington (~7% Black) versus Detroit, Michigan (~75% Black). Finally, the Gi* statistic has been applied fruitfully in several large epidemiological cohort studies on neighborhood segregation and population health disparities.[5,6]

Getis-Ord References

1. Getis A, Ord JK. The Analysis of Spatial Association by Use of Distance Statistics. *Geogr Anal*. 1992;24(3):189-206. doi:10.1111/j.1538-4632.1992.tb00261.x

2. McGowan C, Nanni A, Rydland K, McCoy E, Mullen H, Kershaw K. National Getis-Ord GI* Statistics for Select Populations; 1990-2019. Published online 2022. doi:https://doi.org/10.3886/E170541V3

3. Reardon SF, O'Sullivan D. Measures of Spatial Segregation. *Sociol Methodol*. 2004;34(1):121-162. doi:10.1111/j.0081-1750.2004.00150.x

4. Oka M, Wong DWS. Capturing the Two Dimensions of Residential Segregation at the Neighborhood Level for Health Research. *Front Public Health*. 2014;2. doi:10.3389/fpubh.2014.00118

5. Mayne SL, Hicken MT, Merkin SS, et al. Neighbourhood racial/ethnic residential segregation and cardiometabolic risk: the multiethnic study of atherosclerosis. *J Epidemiol Community Health*. 2019;73(1):26-33. doi:10.1136/jech-2018-211159

6. Kershaw KN, Robinson WR, Gordon-Larsen P, et al. Association of Changes in Neighborhood-Level Racial Residential Segregation With Changes in Blood Pressure Among Black Adults: The CARDIA Study. *JAMA Intern Med*. 2017;177(7):996. doi:10.1001/jamainternmed.2017.1226

Figure S1. Survival Curves: ACL, Waves 1-6 (N = 3,329).

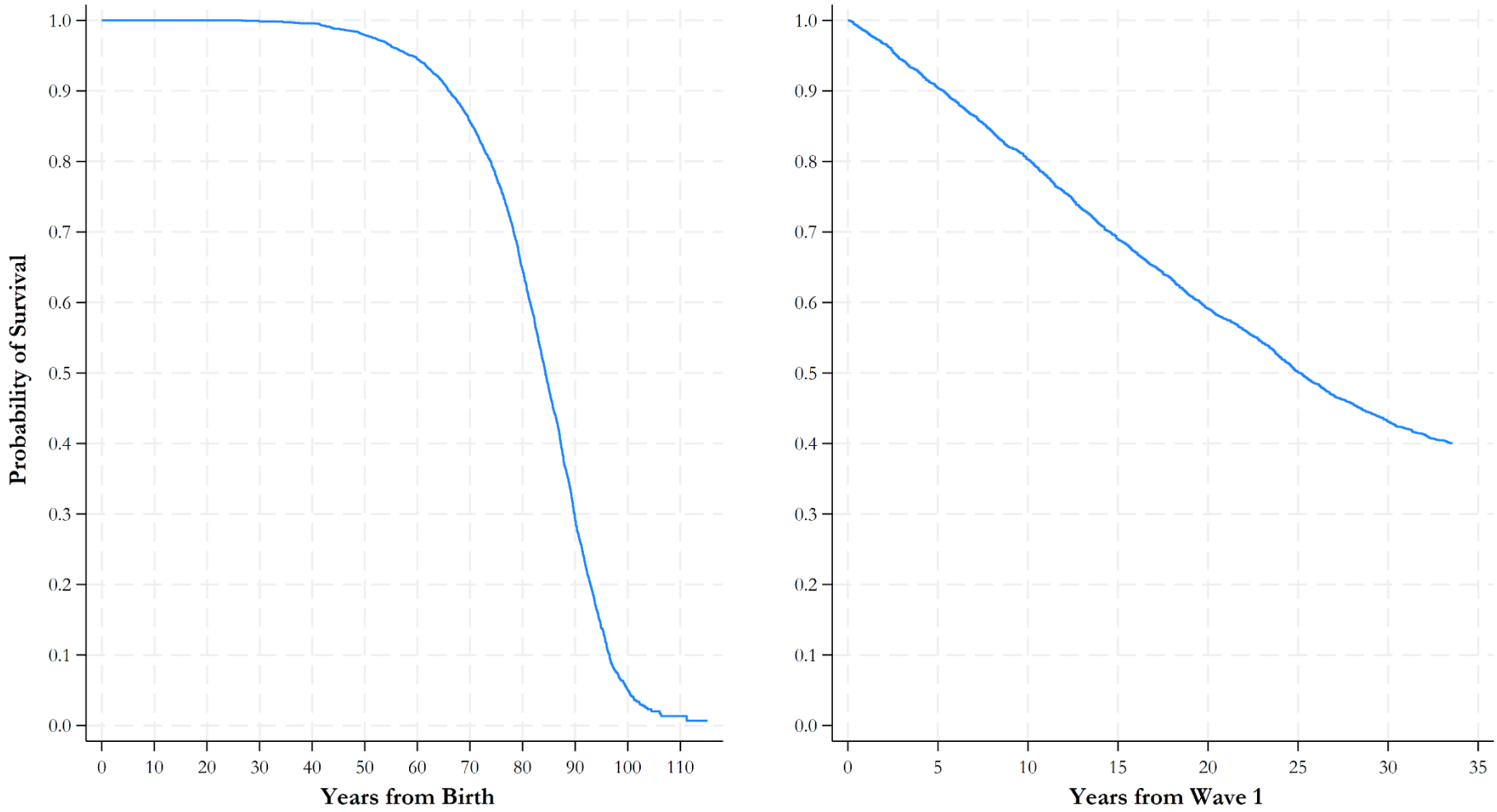

Figure S2. Survival Time in Years from Birth by Logged RSEI Toxicity-Weighted Concentrations: ACL, Waves 1-6 (N = 3,329).

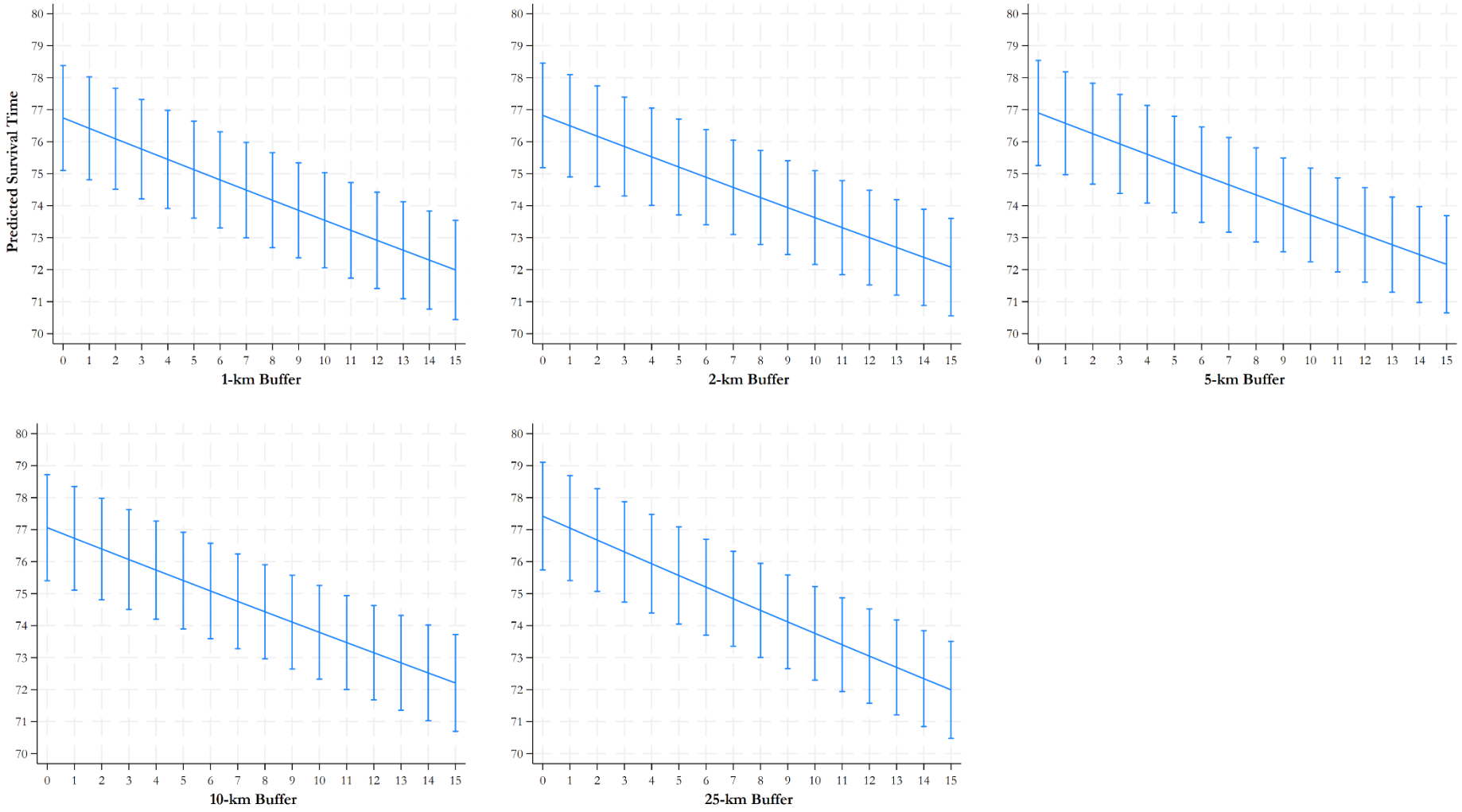

Figure S3. Survival Time in Years from Wave 1 by Logged RSEI Toxicity-Weighted Concentrations: ACL, Waves 1-6 (N = 3,329).

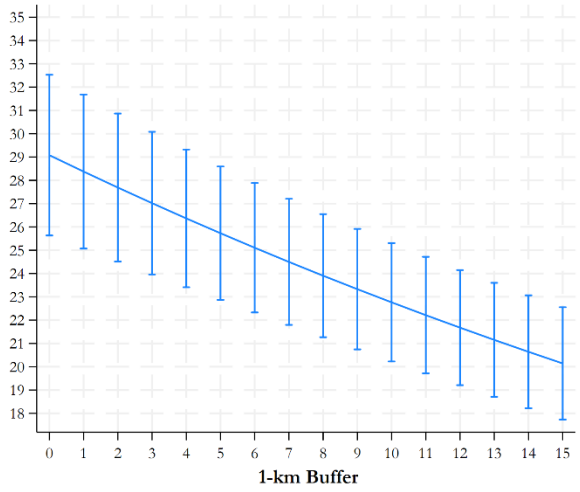

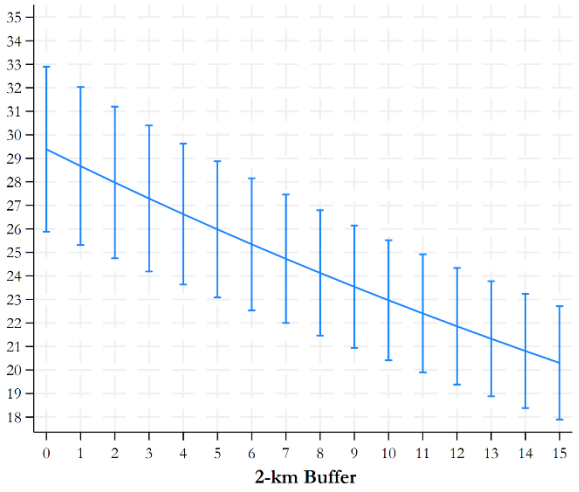

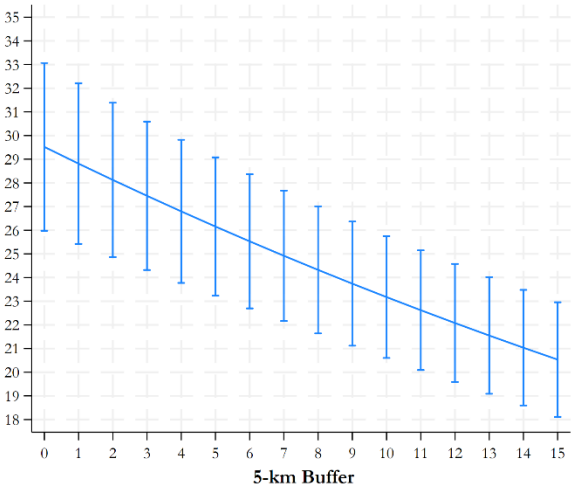

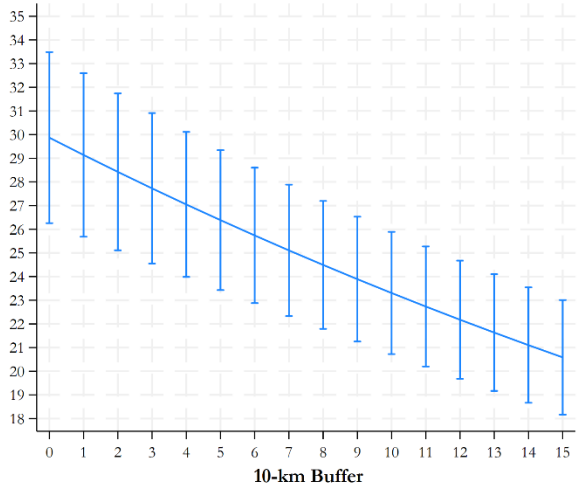

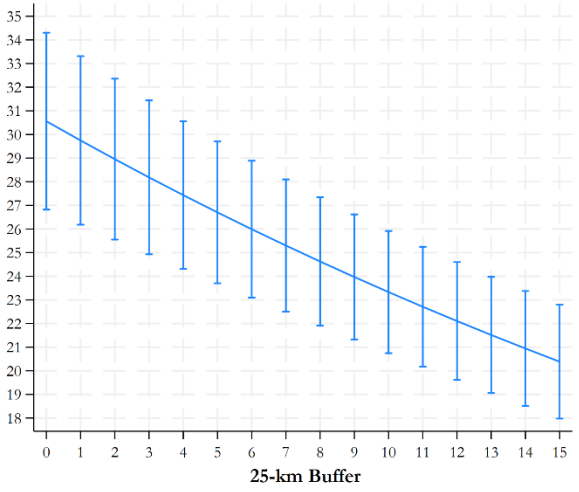

Figure S4. Survival Time in Years from Wave 1 by RSEI Toxicity-Weighted Concentration Splines: ACL, Waves 1-6 (N = 3,329).

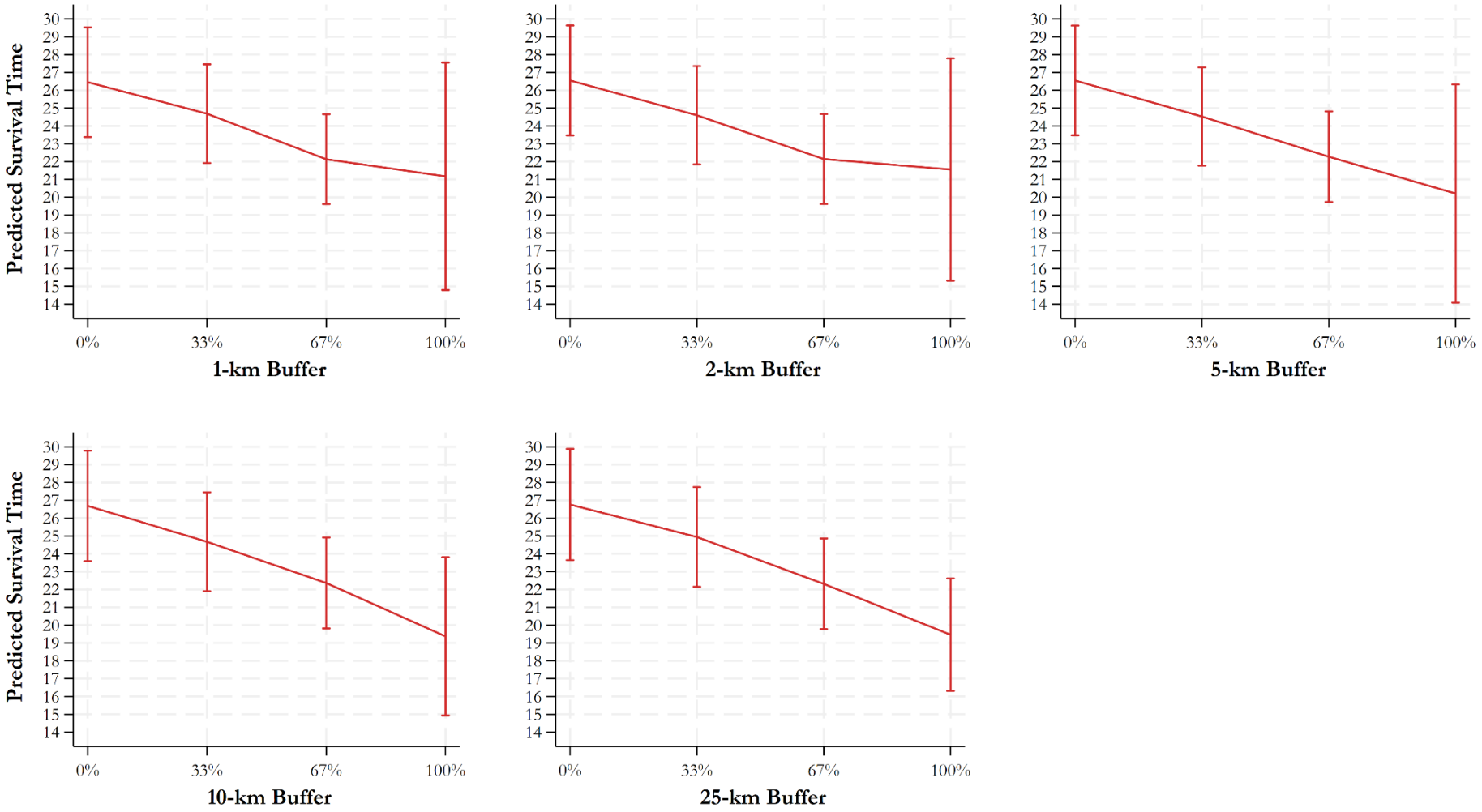

SUPPLEMENTARY TABLES

Table S1. AFT-Shared Frailty Models Testing Interactions with Respondent Race-Ethnicity: ACL, Waves 1-6 (1986-2019; N = 3,329).

	1-km Buffer				2-km Buffer				5-km Buffer			
	Model 1		Model 2		Model 3		Model 4		Model 5		Model 6	
RSEI toxicity-weighted concentrations												
Linear spline @ 0-33%	0.999	*	—		0.999	*	—		0.999	*	—	
	[0.999, 0.999]				[0.999, 0.999]				[0.999, 0.999]			
Linear spline @ 33-67%	0.999	***	—		0.999	***	—		0.999	**	—	
	[0.999, 0.999]				[0.999, 0.999]				[0.999, 0.999]			
Linear spline @ 67-100%	1.000		—		1.000		—		0.999		—	
	[1.000, 1.000]				[1.000, 1.000]				[0.999, 1.000]			
Logged concentration	—		0.996	***	—		0.996	***	—		0.996	***
			[0.995, 0.997]				[0.995, 0.997]				[0.995, 0.998]	
Non-Hispanic Black (vs. White)	0.962	***	0.973	**	0.966	***	0.974	*	0.966	***	0.978	*
	[0.946, 0.977]		[0.954, 0.992]		[0.950, 0.982]		[0.954, 0.994]		[0.951, 0.982]		[0.957, 0.998]	
Hispanic (vs. White)	0.976		0.969		0.977		0.971		0.980		0.973	
	[0.948, 1.005]		[0.939, 1.001]		[0.949, 1.006]		[0.940, 1.004]		[0.952, 1.009]		[0.941, 1.006]	
Interactions: Black												
X Linear spline @ 0-33%	0.999		—		0.999		—		1.000		—	
	[0.999, 1.000]				[0.999, 1.000]				[1.000, 1.000]			
X Linear spline @ 33-67%	1.000		—		1.000		—		1.000		—	
	[1.000, 1.000]				[1.000, 1.000]				[1.000, 1.000]			
X Linear spline @ 67-100%	0.999		—		0.999		—		0.999	*	—	
	[0.999, 1.000]				[0.999, 1.000]				[0.999, 0.999]			
X Logged concentration	—		0.998		—		0.998		—		0.998	
			[0.996, 1.000]				[0.996, 1.000]				[0.996, 1.000]	
Interactions: Hispanic												
X Linear spline @ 0-33%	0.999		—		0.999		—		0.999		—	
	[0.999, 1.000]				[0.999, 1.000]				[0.999, 1.000]			
X Linear spline @ 33-67%	1.000		—		1.000		—		1.000		—	
	[1.000, 1.000]				[1.000, 1.000]				[1.000, 1.000]			
X Linear spline @ 67-100%	1.000		—		1.000		—		1.000		—	
	[1.000, 1.000]				[1.000, 1.000]				[1.000, 1.000]			
X Logged concentration	—		0.998		—		0.998		—		0.998	
			[0.994, 1.001]				[0.994, 1.001]				[0.994, 1.001]	

Note: Models exclude non-Hispanic Asians and Native Americans. Survival time ratios are reported with 95% confidence intervals in brackets; ratios less/greater than 1.00 represent shorter/longer survival times. All estimates account for covariates, five-year birth cohorts, state of residence at each wave, and multiple observations nested within respondents. AFT = accelerated failure time.

*** p<.001, ** p<.01, * p<.05 (two-tailed).

Table S1. Continued.

	10-km Buffer				25-km Buffer			
	Model 7		Model 8		Model 9		Model 10	
RSEI toxicity-weighted concentrations								
Linear spline @ 0-33%	0.999	*	—		0.999	*	—	
	[0.999, 0.999]				[0.999, 0.999]			
Linear spline @ 33-67%	0.999	***	—		0.999	***	—	
	[0.999, 0.999]				[0.999, 0.999]			
Linear spline @ 67-100%	0.999		—		0.999		—	
	[0.999, 1.000]				[0.999, 1.000]			
Logged concentration	—		0.996	***	—		0.996	***
			[0.995, 0.997]				[0.995, 0.997]	
Non-Hispanic Black (vs. White)	0.971	***	0.981		0.968	***	0.986	
	[0.955, 0.988]		[0.960, 1.003]		[0.952, 0.984]		[0.964, 1.009]	
Hispanic (vs. White)	0.981		0.971		0.984		0.969	
	[0.953, 1.011]		[0.938, 1.005]		[0.955, 1.014]		[0.935, 1.005]	
Interactions: Black								
X Linear spline @ 0-33%	0.999		—		0.999		—	
	[0.999, 1.000]				[0.999, 1.000]			
X Linear spline @ 33-67%	1.000		—		0.999		—	
	[1.000, 1.000]				[0.999, 1.000]			
X Linear spline @ 67-100%	0.999		—		0.999		—	
	[0.999, 1.000]				[0.999, 1.000]			
X Logged concentration	—		0.998	*	—		0.997	*
			[0.995, 1.000]				[0.995, 0.999]	
Interactions: Hispanic								
X Linear spline @ 0-33%	0.999		—		0.999	*	—	
	[0.999, 1.000]				[0.999, 1.000]			
X Linear spline @ 33-67%	1.000		—		1.000		—	
	[1.000, 1.000]				[1.000, 1.000]			
X Linear spline @ 67-100%	1.000		—		1.000		—	
	[1.000, 1.000]				[1.000, 1.000]			
X Logged concentration	—		0.998		—		0.999	
			[0.995, 1.002]				[0.995, 1.002]	

Note: Models exclude non-Hispanic Asians and Native Americans. Survival time ratios are reported with 95% confidence intervals in brackets; ratios less/greater than 1.00 represent shorter/longer survival times. All estimates account for covariates, five-year birth cohorts, state of residence at each wave, and multiple observations nested within respondents. AFT = accelerated failure time.

*** p<.001, ** p<.01, * p<.05 (two-tailed).

Table S2. AFT-Shared Frailty Models Testing Interactions with Family Income: ACL, Waves 1-6 (1986-2019; N = 3,402).

	1-km Buffer		2-km Buffer		5-km Buffer	
	Model 1	Model 2	Model 3	Model 4	Model 5	Model 6
RSEI toxicity-weighted concentrations						
Linear spline @ 0-33%	0.999 **	—	0.999 ***	—	0.999 ***	—
	[0.999, 0.999]		[0.999, 0.999]		[0.999, 0.999]	
Linear spline @ 33-67%	0.999 ***	—	0.999 ***	—	0.999 ***	—
	[0.999, 0.999]		[0.999, 0.999]		[0.999, 0.999]	
Linear spline @ 67-100%	1.000	—	0.999	—	0.999	—
	[1.000, 1.000]		[0.999, 1.000]		[0.999, 1.000]	
Logged concentration	—	0.996 ***	—	0.996 ***	—	0.996 ***
		[0.995, 0.997]		[0.995, 0.997]		[0.995, 0.997]
Family income (1000 USD)	1.000	1.000	1.000	1.000	1.000	1.000
	[1.000, 1.000]	[1.000, 1.000]	[1.000, 1.000]	[1.000, 1.000]	[1.000, 1.000]	[1.000, 1.000]
Interactions: Family income						
X Linear spline @ 0-33%	0.999	—	0.999	—	0.999	—
	[0.999, 1.000]		[0.999, 1.000]		[0.999, 1.000]	
X Linear spline @ 33-67%	0.999	—	0.999	—	0.999	—
	[0.999, 1.000]		[0.999, 1.000]		[0.999, 1.000]	
X Linear spline @ 67-100%	1.000	—	1.000	—	1.000	—
	[1.000, 1.000]		[1.000, 1.000]		[1.000, 1.000]	
X Logged concentration	—	0.999	—	0.999	—	0.999
		[0.999, 1.000]		[0.999, 1.000]		[0.999, 1.000]

Note: Survival time ratios are reported with 95% confidence intervals in brackets; ratios less/greater than 1.00 represent shorter/longer survival times. All estimates account for covariates, five-year birth cohorts, state of residence at each wave, and multiple observations nested within respondents. AFT = accelerated failure time. Family income is standardized to 2019 USD to account for inflation.

*** p<.001, ** p<.01, * p<.05 (two-tailed).

Table S2. Continued.

	10-km Buffer				25-km Buffer			
	Model 7		Model 8		Model 9		Model 10	
RSEI toxicity-weighted concentrations								
Linear spline @ 0-33%	0.999	***	—		0.999	*	—	
	[0.999, 0.999]				[0.999, 0.999]			
Linear spline @ 33-67%	0.999	***	—		0.999	***	—	
	[0.999, 0.999]				[0.999, 0.999]			
Linear spline @ 67-100%	0.999	*	—		0.999	*	—	
	[0.999, 0.999]				[0.999, 0.999]			
Logged concentration	—		0.996	***	—		0.995	***
			[0.995, 0.997]				[0.994, 0.996]	
Family income (1000 USD)	1.000		1.000		1.000		1.000	
	[1.000, 1.000]		[1.000, 1.000]		[1.000, 1.000]		[1.000, 1.000]	
Interactions: Family income								
X Linear spline @ 0-33%	0.999		—		0.999		—	
	[0.999, 1.000]				[0.999, 1.000]			
X Linear spline @ 33-67%	0.999		—		0.999		—	
	[0.999, 1.000]				[0.999, 1.000]			
X Linear spline @ 67-100%	1.000	*	—		1.000	*	—	
	[1.000, 1.000]				[1.000, 1.000]			
X Logged concentration	—		0.999		—		0.999	
			[0.999, 1.000]				[0.999, 1.000]	

Note: Survival time ratios are reported with 95% confidence intervals in brackets; ratios less/greater than 1.00 represent shorter/longer survival times. All estimates account for covariates, five-year birth cohorts, state of residence at each wave, and multiple observations nested within respondents. AFT = accelerated failure time. Family income is standardized to 2019 USD to account for inflation.

*** p<.001, ** p<.01, * p<.05 (two-tailed).

Table S3. AFT-Shared Frailty Models Testing Interactions with Tract Poverty: ACL, Waves 1-6 (1986-2019; N = 3,329).

	1-km Buffer		2-km Buffer		5-km Buffer	
	Model 1	Model 2	Model 3	Model 4	Model 5	Model 6
RSEI toxicity-weighted concentrations						
Linear spline @ 0-33%	0.999 **	—	0.999 **	—	0.999 ***	—
	[0.999, 0.999]		[0.999, 0.999]		[0.999, 0.999]	
Linear spline @ 33-67%	0.999 ***	—	0.999 ***	—	0.999 ***	—
	[0.999, 0.999]		[0.999, 0.999]		[0.999, 0.999]	
Linear spline @ 67-100%	1.000	—	1.000	—	0.999	—
	[1.000, 1.000]		[1.000, 1.000]		[0.999, 1.000]	
Logged concentration	—	0.996 ***	—	0.996 ***	—	0.996 ***
		[0.995, 0.997]		[0.995, 0.997]		[0.995, 0.997]
Tract poverty rate	0.998	1.037	0.999	1.040	1.009	1.041
	[0.945, 1.054]	[0.978, 1.099]	[0.946, 1.055]	[0.979, 1.105]	[0.955, 1.067]	[0.977, 1.110]
Interactions: Tract poverty rate						—
X Linear spline @ 0-33%	1.000	—	1.000	—	1.000	
	[1.000, 1.000]		[1.000, 1.000]		[1.000, 1.000]	—
X Linear spline @ 33-67%	0.999	—	0.999	—	0.999	
	[0.999, 1.000]		[0.999, 1.000]		[0.999, 1.000]	—
X Linear spline @ 67-100%	0.999	—	0.999	—	0.999	
	[0.999, 1.000]		[0.999, 1.000]		[0.999, 1.000]	
X Logged concentration	—	0.996	—	0.996	—	0.996
		[0.990, 1.002]		[0.990, 1.002]		[0.990, 1.003]

Note: Survival time ratios are reported with 95% confidence intervals in brackets; ratios less/greater than 1.00 represent shorter/longer survival times. All estimates account for covariates, five-year birth cohorts, state of residence at each wave, and multiple observations nested within respondents. AFT = accelerated failure time.
*** p<.001, ** p<.01, * p<.05 (two-tailed).

Table S3. Continued.

	10-km Buffer				25-km Buffer			
	Model 7		Model 8		Model 9		Model 10	
RSEI toxicity-weighted concentrations								
Linear spline @ 0-33%	0.999	**	—		0.999	**	—	
	[0.999, 0.999]				[0.999, 0.999]			
Linear spline @ 33-67%	0.999	***	—		0.999	***	—	
	[0.999, 0.999]				[0.999, 0.999]			
Linear spline @ 67-100%	0.999		—		0.999	**	—	
	[0.999, 1.000]				[0.999, 0.999]			
Logged concentration	—		0.996	***	—		0.995	***
			[0.995, 0.997]				[0.994, 0.996]	
Tract poverty rate	1.024		1.038		0.996		1.014	
	[0.965, 1.085]		[0.971, 1.110]		[0.947, 1.048]		[0.949, 1.082]	
Interactions								
Tract poverty X Linear spline @ 0-33%	0.999		—		1.000		—	
	[0.999, 1.000]				[1.000, 1.000]			
Tract poverty X Linear spline @ 33-67%	0.999		—		1.000		—	
	[0.999, 1.000]				[1.000, 1.000]			
Tract poverty X Linear spline @ 67-100%	0.999		—		0.999	*	—	
	[0.999, 1.000]				[0.999, 0.999]			
Tract poverty X Logged score	—		0.996		—		0.998	
			[0.990, 1.003]				[0.991, 1.005]	

Note: Survival time ratios are reported with 95% confidence intervals in brackets; ratios less/greater than 1.00 represent shorter/longer survival times. All estimates account for covariates, five-year birth cohorts, state of residence at each wave, and multiple observations nested within respondents. AFT = accelerated failure time. RSEI toxicity-weighted concentration is divided by 1,000 to facilitate coefficient interpretation.
*** p<.001, ** p<.01, * p<.05 (two-tailed).

Table S4. AFT-Shared Frailty Models Testing Interactions with Black Tract Segregation: ACL, Waves 1-6 (1986-2019; N = 3,329).

	1-km Buffer				2-km Buffer			
	Model 1		Model 2		Model 3		Model 4	
RSEI toxicity-weighted concentrations								
Linear spline @ 0-33%	0.999	**	—		0.999	**	—	
	[0.999, 0.999]				[0.999, 0.999]			
Linear spline @ 33-67%	0.999	***	—		0.999	***	—	
	[0.999, 0.999]				[0.999, 0.999]			
Linear spline @ 67-100%	1.000		—		1.000		—	
	[1.000, 1.000]				[1.000, 1.000]			
Logged concentration	—		0.996	***	—		0.996	***
			[0.995, 0.997]				[0.995, 0.997]	
Segregated Black tract (vs. not)	0.998		1.013		0.998		1.013	
	[0.978, 1.019]		[0.992, 1.036]		[0.978, 1.019]		[0.990, 1.036]	
Interactions: Segregated Black tract								
X Linear spline @ 0-33%	1.000		—		1.000		—	
	[1.000, 1.000]				[1.000, 1.000]			
X Linear spline @ 33-67%	0.999		—		0.999		—	
	[0.999, 1.000]				[0.999, 1.000]			
X Linear spline @ 67-100%	0.999		—		0.999		—	
	[0.999, 1.000]				[0.999, 1.000]			
X Logged concentration	—		0.998		—		0.998	
			[0.996, 1.000]				[0.996, 1.000]	

Note: Survival time ratios are reported with 95% confidence intervals in brackets; ratios less/greater than 1.00 represent shorter/longer survival times. All estimates account for covariates, five-year birth cohorts, state of residence at each wave, and multiple observations nested within respondents. AFT = accelerated failure time.

*** p<.001, ** p<.01 (two-tailed).

Table S4. Continued.

	5-km Buffer		10-km Buffer		25-km Buffer	
	Model 5	Model 6	Model 7	Model 8	Model 9	Model 10
RSEI toxicity-weighted concentrations						
Linear spline @ 0-33%	0.999 ***	—	0.999 ***	—	0.999 **	—
	[0.999, 0.999]		[0.999, 0.999]		[0.999, 0.999]	
Linear spline @ 33-67%	0.999 **	—	0.999 **	—	0.999 ***	—
	[0.999, 0.999]		[0.999, 0.999]		[0.999, 0.999]	
Linear spline @ 67-100%	0.999	—	0.999	—	0.999	—
	[0.999, 1.000]		[0.999, 1.000]		[0.999, 1.000]	
Logged concentration	—	0.996 ***	—	0.996 ***	—	0.995 ***
		[0.995, 0.997]		[0.995, 0.997]		[0.994, 0.997]
Segregated Black tract (vs. not)	0.999	1.013	0.994	1.011	0.993	1.013
	[0.979, 1.020]	[0.989, 1.036]	[0.973, 1.015]	[0.987, 1.036]	[0.974, 1.012]	[0.989, 1.037]
Interactions: Segregated Black tract						
X Linear spline @ 0-33%	0.999	—	1.000	—	1.000	—
	[0.999, 1.000]		[1.000, 1.000]		[1.000, 1.000]	
X Linear spline @ 33-67%	0.999	—	0.999	—	0.999	—
	[0.999, 1.000]		[0.999, 1.000]		[0.999, 1.000]	
X Linear spline @ 67-100%	0.999	—	0.999	—	0.999	—
	[0.999, 1.000]		[0.999, 1.000]		[0.999, 1.000]	
X Logged concentration	—	0.998	—	0.998	—	0.998
		[0.996, 1.000]		[0.996, 1.001]		[0.996, 1.001]

Note: Survival time ratios are reported with 95% confidence intervals in brackets; ratios less/greater than 1.00 represent shorter/longer survival times. All estimates account for covariates, five-year birth cohorts, state of residence at each wave, and multiple observations nested within respondents. AFT = accelerated failure time.

*** p<.001, ** p<.01 (two-tailed).

Table S5. AFT-Shared Frailty Models Testing Interactions with Hispanic Tract Segregation: ACL, Waves 1-6 (1986-2019; N = 3,329).

	1-km Buffer				2-km Buffer			
	Model 1		Model 2		Model 3		Model 4	
RSEI toxicity-weighted concentrations								
Linear spline @ 0-33%	0.999	**	—		0.999	**	—	
	[0.999, 0.999]				[0.999, 0.999]			
Linear spline @ 33-67%	0.999	***	—		0.999	***	—	
	[0.999, 0.999]				[0.999, 0.999]			
Linear spline @ 67-100%	1.000		—		0.999		—	
	[1.000, 1.000]				[0.999, 1.000]			
Logged concentration	—		0.996	***	—		0.996	***
			[0.995, 0.997]				[0.995, 0.997]	
Segregated Hispanic tract (vs. not)	0.999		1.000		0.999		1.002	
	[0.977, 1.022]		[0.975, 1.026]		[0.976, 1.023]		[0.976, 1.029]	
Interactions: Segregated Hispanic tract								
X Linear spline @ 0-33%	1.000		—		1.000		—	
	[1.000, 1.000]				[1.000, 1.000]			
X Linear spline @ 33-67%	1.000		—		1.000		—	
	[1.000, 1.000]				[1.000, 1.000]			
X Linear spline @ 67-100%	1.000		—		1.000		—	
	[1.000, 1.000]				[1.000, 1.000]			
X Logged concentration	—		1.000		—		1.000	
			[0.997, 1.003]				[0.997, 1.003]	

Note: Survival time ratios are reported with 95% confidence intervals in brackets; ratios less/greater than 1.00 represent shorter/longer survival times. All estimates account for covariates, five-year birth cohorts, state of residence at each wave, and multiple observations nested within respondents. AFT = accelerated failure time.

*** p<.001, ** p<.01 (two-tailed).

Table S5. Continued.

	5-km Buffer			10-km Buffer			25-km Buffer		
	Model 5		Model 6	Model 7		Model 8	Model 9		Model 10
RSEI toxicity-weighted concentrations									
Linear spline @ 0-33%	0.999	***	—	0.999	***	—	0.999	**	—
	[0.999, 0.999]			[0.999, 0.999]			[0.999, 0.999]		
Linear spline @ 33-67%	0.999	***	—	0.999	***	—	0.999	***	—
	[0.999, 0.999]			[0.999, 0.999]			[0.999, 0.999]		
Linear spline @ 67-100%	0.999		—	0.999	*	—	1.000	**	—
	[0.999, 1.000]			[0.999, 0.999]			[1.000, 1.000]		
Logged concentration	—		0.996 ***	—		0.996 ***	—		0.995 ***
			[0.995, 0.997]			[0.995, 0.997]			[0.994, 0.996]
Segregated Hispanic tract (vs. not)	1.001		1.002	0.995		1.005	0.982		0.999
	[0.978, 1.024]		[0.973, 1.031]	[0.971, 1.019]		[0.975, 1.036]	[0.959, 1.005]		[0.967, 1.032]
Interactions: Segregated Hispanic tract									
X Linear spline @ 0-33%	1.000		—	1.000		—	1.000		—
	[1.000, 1.000]			[1.000, 1.000]			[1.000, 1.000]		
X Linear spline @ 33-67%	1.000		—	1.000		—	1.000		—
	[1.000, 1.000]			[1.000, 1.000]			[1.000, 1.000]		
X Linear spline @ 67-100%	1.000		—	1.000		—	1.000		—
	[1.000, 1.000]			[1.000, 1.000]			[1.000, 1.000]		
X Logged concentration	—		1.000	—		1.000	—		1.000
			[0.997, 1.003]			[0.997, 1.003]			[0.997, 1.004]

Note: Survival time ratios are reported with 95% confidence intervals in brackets; ratios less/greater than 1.00 represent shorter/longer survival times. All estimates account for covariates, five-year birth cohorts, state of residence at each wave, and multiple observations nested within respondents. AFT = accelerated failure time.

*** p<.001, ** p<.01 (two-tailed).

Table S6. AFT Models of Survival Time from Birth with Respondent-Level Clustered Standard Errors: Testing Sensitivity to Survey Weights, ACL Waves 1-6 (1986-2019).

	1-km Buffer				2-km Buffer			
	Weighted	Unweighted	Weighted	Unweighted	Weighted	Unweighted	Weighted	Unweighted
RSEI Toxicity-Weighted Concentrations (logged)	0.992 ***	0.992 ***	—	—	0.992 ***	0.992 ***	—	—
	[0.989, 0.995]	[0.991, 0.994]			[0.989, 0.995]	[0.991, 0.994]		
Linear spline @ 0-33%	—	—	0.999 **	0.999 **	—	—	0.999 **	0.999 ***
			[0.999, 0.999]	[0.999, 0.999]			[0.999, 0.999]	[0.999, 0.999]
Linear spline @ 33-67%	—	—	0.999 ***	0.999 ***	—	—	0.999 ***	0.999 ***
			[0.999, 0.999]	[0.999, 0.999]			[0.999, 0.999]	[0.999, 0.999]
Linear spline @ 67-100%	—	—	0.999	0.999	—	—	1.000	0.999
			[0.999, 1.000]	[0.999, 1.000]			[0.999, 1.000]	[0.999, 1.000]
Intercept	83.247 ***	83.547 ***	81.443 ***	81.519 ***	83.454 ***	83.790 ***	81.489 ***	81.624 ***
	[78.648, 88.115]	[80.577, 86.627]	[76.957, 86.189]	[78.648, 84.494]	[78.824, 88.357]	[80.793, 86.898]	[77.002, 86.238]	[78.757, 84.595]
Number of observations	11439	11439	11439	11439	11440	11440	11440	11440

Note: Survival time ratios are reported with 95% confidence intervals in brackets; ratios less/greater than 1.00 represent shorter/longer survival times. All estimates account for covariates, state of residence at each wave, five-year birth cohorts, and robust standard errors clustered at the respondent level. Weighted estimates incorporate baseline ACL survey weights (V1860). AFT = accelerated failure time.

*** p<.001, ** p<.01, * p<.05 (two-tailed).

Table S6. Continued.

	5-km Buffer				10-km Buffer			
	Weighted	Unweighted	Weighted	Unweighted	Weighted	Unweighted	Weighted	Unweighted
RSEI Toxicity-Weighted Concentrations (logged)	0.992 ***	0.993 ***	—	—	0.992 ***	0.992 ***	—	—
	[0.989, 0.995]	[0.991, 0.995]			[0.989, 0.995]	[0.991, 0.994]		
Linear spline @ 0-33%	—	—	0.999 **	0.999 ***	—	—	0.999 **	0.999 ***
			[0.999, 0.999]	[0.999, 0.999]			[0.999, 0.999]	[0.999, 0.999]
Linear spline @ 33-67%	—	—	0.999 ***	0.999 ***	—	—	0.999 ***	0.999 ***
			[0.999, 0.999]	[0.999, 0.999]			[0.999, 0.999]	[0.999, 0.999]
Linear spline @ 67-100%	—	—	0.999	0.999	—	—	1.000	0.999
			[0.999, 1.000]	[0.999, 1.000]			[0.999, 1.000]	[0.999, 1.000]
Intercept	83.557 ***	83.884 ***	81.575 ***	82.197 ***	83.855 ***	84.147 ***	81.613 ***	81.911 ***
	[78.904, 88.485]	[80.868, 87.012]	[77.094, 86.317]	[79.311, 85.187]	[79.171, 88.816]	[81.110, 87.297]	[77.114, 86.374]	[79.030, 84.897]
Number of observations	11444	11444	11444	11444	11445	11445	11445	11445

Note: Survival time ratios are reported with 95% confidence intervals in brackets; ratios less/greater than 1.00 represent shorter/longer survival times. All estimates account for covariates, state of residence at each wave, five-year birth cohorts, and robust standard errors clustered at the respondent level. Weighted estimates incorporate baseline ACL survey weights (V1860). AFT = accelerated failure time.
*** p<.001, ** p<.01, * p<.05 (two-tailed).

Table S6. Continued.

	25-km Buffer							
	Weighted		Unweighted		Weighted		Unweighted	
RSEI Toxicity-Weighted Concentrations (logged)	0.991	***	0.992	***	—		—	
	[0.988, 0.995]		[0.990, 0.994]					
Linear spline @ 0-33%	—		—		0.999	*	0.999	***
					[0.999, 0.999]		[0.999, 0.999]	
Linear spline @ 33-67%	—		—		0.999	***	0.999	***
					[0.999, 0.999]		[0.999, 0.999]	
Linear spline @ 67-100%	—		—		1.000		0.999	
					[0.999, 1.000]		[0.999, 1.000]	
Intercept	84.351	***	84.473	***	81.345	***	81.668	***
	[79.584, 89.403]		[81.397, 87.664]		[76.834, 86.120]		[78.797, 84.644]	
Number of observations	11452		11452		11452		11452	

Note: Survival time ratios are reported with 95% confidence intervals in brackets; ratios less/greater than 1.00 represent shorter/longer survival times. All estimates account for covariates, state of residence at each wave, five-year birth cohorts, and robust standard errors clustered at the respondent level. Weighted estimates incorporate baseline ACL survey weights (V1860). AFT = accelerated failure time.

*** p<.001, ** p<.01, * p<.05 (two-tailed).

Table S7. AFT-Shared Frailty Models of Survival Time from Wave 1: ACL, Waves 1-6 (1986-2019; N = 3,329).

	1-km	2-km	5-km	10-km	25-km
RSEI toxicity-weighted concentrations					
Linear spline @ 0-33%	0.999 **	0.999 **	0.999 **	0.999 **	0.999 **
	[0.999, 0.999]	[0.999, 0.999]	[0.999, 0.999]	[0.999, 0.999]	[0.999, 0.999]
Linear spline @ 33-67%	0.999 ***	0.999 ***	0.999 ***	0.999 ***	0.999 ***
	[0.999, 0.999]	[0.999, 0.999]	[0.999, 0.999]	[0.999, 0.999]	[0.999, 0.999]
Linear spline @ 67-100%	0.999	0.999	0.999	0.999	0.999 *
	[0.999, 1.000]	[0.999, 1.000]	[0.999, 1.000]	[0.999, 1.000]	[0.999, 1.000]
Non-Hispanic Black (vs. non-Hispanic White)	0.744 ***	0.745 ***	0.746 ***	0.748 ***	0.751 ***
	[0.706, 0.784]	[0.707, 0.785]	[0.708, 0.786]	[0.710, 0.788]	[0.713, 0.791]
Hispanic (vs. non-Hispanic White)	0.812 ***	0.812 ***	0.811 ***	0.813 ***	0.825 ***
	[0.727, 0.909]	[0.726, 0.908]	[0.725, 0.907]	[0.727, 0.909]	[0.738, 0.922]
Female (vs. male)	1.236 ***	1.236 ***	1.236 ***	1.235 ***	1.237 ***
	[1.187, 1.287]	[1.187, 1.287]	[1.187, 1.287]	[1.186, 1.286]	[1.188, 1.287]
Married (vs. not married)	1.000	1.000	1.000	1.001	1.002
	[0.969, 1.032]	[0.969, 1.033]	[0.969, 1.032]	[0.970, 1.033]	[0.971, 1.034]
College degree (vs. less)	1.118 ***	1.118 ***	1.119 ***	1.119 ***	1.121 ***
	[1.054, 1.185]	[1.055, 1.185]	[1.055, 1.186]	[1.056, 1.187]	[1.057, 1.188]
Employed (vs. non-employed/disabled)	1.039 *	1.039 *	1.037 *	1.038 *	1.040 *
	[1.007, 1.071]	[1.007, 1.071]	[1.006, 1.069]	[1.007, 1.070]	[1.009, 1.072]
Family income (1000 USD)	1.000	1.000	1.000	1.000	1.000
	[1.000, 1.000]	[1.000, 1.000]	[1.000, 1.000]	[1.000, 1.000]	[1.000, 1.000]
Homeowner (vs. not)	1.067 ***	1.067 ***	1.066 ***	1.064 ***	1.062 ***
	[1.030, 1.105]	[1.030, 1.105]	[1.029, 1.105]	[1.027, 1.103]	[1.025, 1.100]
Never smoked (vs. current/former smoker)	1.252 ***	1.252 ***	1.252 ***	1.252 ***	1.254 ***
	[1.205, 1.300]	[1.206, 1.301]	[1.206, 1.301]	[1.206, 1.301]	[1.207, 1.302]
Recently moved (vs. same residence)	0.983	0.980	0.981	0.972	0.940
	[0.852, 1.134]	[0.849, 1.131]	[0.850, 1.131]	[0.843, 1.121]	[0.815, 1.085]
Tract poverty rate	1.006	1.005	1.003	1.005	1.008
	[0.957, 1.057]	[0.956, 1.057]	[0.955, 1.055]	[0.956, 1.056]	[0.959, 1.059]
Segregated Black tract (vs. not)	1.016	1.017	1.017	1.016	1.014
	[0.966, 1.067]	[0.968, 1.069]	[0.968, 1.069]	[0.967, 1.068]	[0.964, 1.065]
Segregated Hispanic tract (vs. not)	1.077 **	1.078 ***	1.077 **	1.074 **	1.075 **
	[1.030, 1.125]	[1.031, 1.126]	[1.030, 1.125]	[1.028, 1.122]	[1.029, 1.123]
Metro area (vs. small town/rural)	1.011	1.011	1.011	1.010	1.008
	[0.980, 1.043]	[0.980, 1.043]	[0.980, 1.043]	[0.979, 1.042]	[0.977, 1.040]
Intercept	18.443 ***	18.493 ***	18.503 ***	18.578 ***	18.574 ***
	[16.498, 20.618]	[16.543, 20.672]	[16.555, 20.680]	[16.619, 20.767]	[16.605, 20.776]
Theta	3.497	3.496	3.502	3.501	3.524
	[3.188, 3.836]	[3.187, 3.835]	[3.193, 3.842]	[3.192, 3.840]	[3.214, 3.865]

Note: Survival time ratios are reported with 95% confidence intervals in brackets; ratios less/greater than 1.00 represent shorter/longer survival times. All estimates account for multiple observations per respondent, five-year birth cohorts, and state of residence at each wave. Family income is standardized to 2019 USD at each wave to account for inflation. Family income and tract poverty rate are centered on their sample means. AFT = accelerated failure time. Theta = estimated frailty variance.

*** p<.001, ** p<.01, * p<.05 (two-tailed).

Table S8. AFT-Shared Frailty Models Excluding External/Unknown Causes of Death: ACL, Waves 1-6 (1986-2019; N = 3,276).

	1-km Buffer		2-km Buffer		5-km Buffer		10-km Buffer		25-km Buffer	
RSEI toxicity-weighted concentrations										
Linear spline @ 0-33%	0.999	**	0.999	***	0.999	***	0.999	***	0.999	**
	[0.999, 0.999]		[0.999, 0.999]		[0.999, 0.999]		[0.999, 0.999]		[0.999, 0.999]	
Linear spline @ 33-67%	0.999	***	0.999	***	0.999	***	0.999	***	0.999	***
	[0.999, 0.999]		[0.999, 0.999]		[0.999, 0.999]		[0.999, 0.999]		[0.999, 0.999]	
Linear spline @ 67-100%	1.000		0.999		0.999		0.999		0.999	**
	[0.999, 1.000]		[0.999, 1.000]		[0.999, 1.000]		[0.999, 1.000]		[0.999, 0.999]	
Intercept	77.928	***	77.963	***	78.081	***	78.089	***	78.057	***
	[76.448, 79.436]		[76.483, 79.471]		[76.570, 79.621]		[76.586, 79.623]		[76.561, 79.582]	
Theta	7.026		7.025		6.866		6.930		7.041	
	[6.536, 7.553]		[6.535, 7.552]		[6.384, 7.384]		[6.444, 7.452]		[6.550, 7.568]	

Note: Survival time ratios are reported with 95% confidence intervals in brackets; ratios less/greater than 1.00 represent shorter/longer survival times. All estimates account for covariates, five-year birth cohorts, state of residence at each wave, and multiple observations nested within respondents. AFT = accelerated failure time. Theta = estimated frailty variance.

*** p<.001, ** p<.01, * p<.05 (two-tailed).